


# In Vivo and In Vitro Evaluation of a Novel Hyaluronic Acid–Laminin Hydrogel as Luminal Filler and Carrier System for Genetically Engineered Schwann Cells in Critical Gap Length Tubular Peripheral Nerve Graft in Rats

Nina Dietzmeyer<sup>1,2</sup> , Zhong Huang<sup>1,2</sup>, Tobias Schüning<sup>1,2</sup>, Shimon Rochkind<sup>3</sup>, Mara Almog<sup>3</sup>, Zvi Nevo(†)<sup>4</sup>, Thorsten Lieke<sup>5</sup>, Svenja Kankowski<sup>1</sup>, and Kirsten Haastert-Talini<sup>1,2</sup>

Cell Transplantation  
Volume 29: 1–20  
© The Author(s) 2020  
Article reuse guidelines:  
sagepub.com/journals-permissions  
DOI: 10.1177/0963689720910095  
journals.sagepub.com/home/ctj  


## Abstract

In the current study we investigated the suitability of a novel hyaluronic acid–laminin hydrogel (HAL) as luminal filler and carrier system for co-transplanted cells within a composite chitosan-based nerve graft (CNG) in a rat critical nerve defect model. The HAL was meant to improve the performance of our artificial nerve guides by giving additional structural and molecular support to regrowing axons. We filled hollow CNGs or two-chambered nerve guides with an inserted longitudinal chitosan film (CNG[F]s), with cell-free HAL or cell-free HA or additionally suspended either naïve Schwann cells (SCs) or fibroblast growth factor 2-overexpressing Schwann cells (FGF2-SCs) within the gels. We subjected female Lewis rats to immediate 15 mm sciatic nerve gap reconstruction and comprehensively compared axonal and functional regeneration parameters with the gold standard autologous nerve graft (ANG) repair. Motor recovery was surveyed by means of electrodiagnostic measurements at 60, 90, and 120 days post-reconstruction. Upon explantation after 120 days, lower limb target muscles were harvested for calculation of muscle-weight ratios. Semi-thin cross-sections of nerve segments distal to the grafts were evaluated histomorphometrically. After 120 days of recovery, only ANG treatment led to full motor recovery. Surprisingly, regeneration outcomes revealed no regeneration-supportive effect of HAL alone and even an impairment of peripheral nerve regeneration when combined with SCs and FGF2-SCs. Furthermore, complementary in vitro studies, conducted to elucidate the reason for this unexpected negative result, revealed that SCs and FGF2-SCs suspended within the hydrogel relatively downregulated gene expression of regeneration-supporting neurotrophic factors. In conclusion, cell-free HAL in its current formulation did not qualify for optimizing regeneration outcome through CNG[F]s. In addition, we demonstrate that our HAL, when used as a carrier system for co-transplanted SCs, changed their gene expression profile and deteriorated the pro-regenerative milieu within the nerve guides.

## Keywords

cellular drug delivery system, Schwann cells, sciatic nerve regeneration, fibroblast growth factor 2, chitosan

<sup>1</sup> Institute of Neuroanatomy and Cell Biology, Hannover Medical School, Hannover, Germany

<sup>2</sup> Center for Systems Neuroscience, Hannover, Germany

<sup>3</sup> Research Center for Nerve Reconstruction, Department of Neurosurgery, Tel-Aviv Sourasky Medical Center, Tel Aviv University, Tel Aviv, Israel

<sup>4</sup> Department of Human Molecular Genetics and Biochemistry, Sackler School of Medicine, Tel Aviv University, Tel Aviv, Israel

<sup>5</sup> Transplant Laboratory, Department of General-, Visceral-, and Transplantation Surgery, Hannover Medical School, Hannover, Germany

Submitted: December 21, 2019. Revised: February 04, 2020. Accepted: February 10, 2020.

†Prof. Nevo passed away

## Corresponding Author:

Kirsten Haastert-Talini, Hannover Medical School, Carl-Neuberg-Str. 1, Hannover 30625, Germany.

Email: Haastert-talini.Kirsten@mh-hannover.de



Creative Commons Non Commercial CC BY-NC: This article is distributed under the terms of the Creative Commons Attribution-NonCommercial 4.0 License (<https://creativecommons.org/licenses/by-nc/4.0/>) which permits non-commercial use, reproduction and distribution of the work without further permission provided the original work is attributed as specified on the SAGE and Open Access pages (<https://us.sagepub.com/en-us/nam/open-access-at-sage>).

## Introduction

Injuries of peripheral nerves (PNIs) annually affect more than one million people worldwide<sup>1</sup>. Resulting in partial or complete paralyses of the innervated muscles, traumatic PNIs may even lead to persisting severe pain and/or numbness. A reduced quality of life, overall performance, and lifelong dependency on support are serious consequences for the affected patients<sup>2,3</sup>. Despite modern microsurgical treatment techniques only a maximum of about 50% of the patients regain good-to-excellent motor function<sup>4</sup>. The mostly young- to middle-aged patients are not able to reenter their full work routine. Thus, the socioeconomic impact of PNIs is not negligible<sup>5</sup>.

Until now, the gold standard microsurgical treatment approach is the use of autologous nerve grafts (ANGs)<sup>4</sup>. Besides not guaranteeing full functional recovery, e.g., as a result of incorrect target reinnervation, the use of ANGs goes along with several other downsides, such as donor site morbidity, the need for polysurgery, and a limited availability of donor tissue especially for extended injuries of the brachial plexus<sup>6</sup>. To circumvent these downsides, several off-the-shelf artificial nerve grafts are available for clinical use<sup>7</sup>. However, artificial nerve grafts are only approved as grafting material for gap lengths up to 3 cm<sup>7-10</sup>.

The development of novel treatment strategies for bridging longer peripheral nerve defects still remains a major challenge in human medicine. Therefore, researchers aim at designing bioartificial nerve grafts that best mimic the natural milieu of the original nerve structure in order to provide regeneration-supportive cues<sup>7,11-13</sup>. Schwann cells (SCs) are key players in the process of degeneration and regeneration upon complete transection injury of a peripheral nerve (neurotmesis)<sup>5,14</sup>. Reprogrammed to a repair phenotype, SCs are able to downregulate the expression of myelin genes and, on the other hand, to up- or downregulate gene expression of neurotrophic factors, which upon their release serve as chemoattractant and support proteins for the regrowing axons<sup>15</sup>. Another key component during regeneration after PNI is the extracellular matrix (ECM). As a three-dimensional matrix it drives regeneration and promotes axonal growth and guidance through gathering activating elements for the regeneration-associated signaling pathways<sup>16</sup>. Furthermore, whenever the basal lamina of the endoneurial tubes, as part of the ECM in the peripheral nerve, does not remain intact to guide the axons back to the target tissue, SCs increase the production of ECM molecules forming the basal lamina and the Bands of Büngner for undertaking the guidance of the axonal growth cone<sup>16,17</sup>.

In the recent past, we demonstrated that chitosan-based hollow nerve guidance channels (CNGs) allow effective regeneration in rat models when bridging 10 mm rat sciatic nerve gaps<sup>18,19</sup>. Hollow nerve guides (CNGs) did even allow functional repair across 15 mm critical length sciatic nerve gaps in a considerably high percentage of rats<sup>20</sup>. The performance of the nerve guides in the repair of acute and delayed

nerve repair was even increased by transforming them into two-chambered tubular grafts with the introduction of a longitudinal chitosan film (CNG[F]s)<sup>21,22</sup>. Although these developments have been promising, there is an emerging consensus that for becoming a reliable substitute for autologous nerve grafting in long gap repair, a permissive scaffold should have enhanced properties for axonal guidance and for neurotrophic support<sup>7</sup>. Co-transplanted SCs of primary origin are genetically modified to overexpress neurotrophic factors<sup>23,24</sup> and growth-permissive substrates such as hydrogels could be a solution to this. In one of our previous studies, we have therefore already filled CNGs with another hydrogel with a different composition of high-molecular-weight hyaluronic acid (HA) and laminin in a non modified form or enriched with either primary, naïve SCs or genetically modified SCs overexpressing neurotrophic factors<sup>25</sup>. Surprising to us, the attempt to fill the nerve guide with the specific hydrogel did not provide a growth-permissive environment *in vivo*, but it rather impaired the regeneration process and only the co-transplantation of fibroblast growth factor 2 (FGF-2)-overexpressing SCs (FGF2-SCs) partially resolved this problem<sup>25</sup>. FGF-2 has been a promising candidate for regenerative strategies, because its expression is increased within hours following nerve crush<sup>26</sup>. It is further known to affect axonal outgrowth across nerve crush lesions<sup>27</sup>, to increase regeneration through peripheral nerve guides<sup>28-30</sup>, and to play a crucial role for the development of the substantia nigra and the rescue of dopaminergic neurons in models of Parkinson's disease<sup>31</sup>. In another previous approach, we have seeded naïve SCs or FGF2-SCs into CNG[F]s, without adding any hydrogel, and again used them for repairing critical length sciatic nerve defects in the rat<sup>21</sup>. In this approach, however, the FGF2-SCs had no additional regeneration-supporting effect and we concluded that they would have needed to be surrounded by an appropriate matrix at the time of implantation<sup>21</sup>.

In the current study, we hypothesized that another novel hyaluronic acid-laminin hydrogel (HAL) could serve as a luminal filler for CNGs or CNG[F]s and as a carrier system for co-transplanted SCs or FGF2-SCs. The novel HAL has been modified from another previous study, in which a similar hydrogel, differing in the concentration of HA, was filled into a collagen-based nerve guidance channel and enabled axonal regeneration across a 15-mm Wistar rat sciatic nerve gap, while the empty channel failed to do so<sup>32</sup>.

To test our hypothesis, we have comprehensively evaluated *in vivo* the potential of CNGs or CNG[F]s filled with only hydrogel, in this case HA or HAL, or filled with SCs or FGF-SCs carrying hydrogel to support axonal regeneration across a critical defect size of 15 mm in the rat sciatic nerve and to subsequently allow functional motor recovery. A total of eight artificial nerve graft treated animal groups were compared to one group that was treated with the gold standard, reversed nerve autograft.

Our comprehensive *in vivo* evaluation revealed that cell-free HA or HAL has an equal potential to support

regeneration through hollow CNGs and that regeneration outcome is improved when applying CNG[F]s. Interestingly, we detected that adding cells to the system did dramatically reduce the regeneration outcome, especially when using HAL as a cell carrier system. To elucidate what might be the reason for this, we further present some *in vitro* and gene expression analyses.

## Materials and Methods

### Primary (Naive) Neonatal Rat SCs

Primary neonatal rat SCs were cultured according to a previously published work<sup>33</sup>. Roughly summarized, we used Wistar RjHan:WI rat pups (P1-3, in-house breeding) to obtain the sciatic nerves. The nerves were enzymatically digested for 50 min and afterwards mechanically dissociated. Isolated cells were cultured for 24 h in culture medium [Dulbecco's modified Eagle's medium, 0.1 mM Forskolin, 1% Pen/strep, 2 mM L-glutamine, 1 mM sodium pyruvate, and 10% fetal calf serum (FCS); all from Thermo Fisher Scientific, Waltham, MA, USA]. After 24 h half of the medium was refreshed and 1 mM of arabinoside-c (Sigma-Aldrich, St. Louis, MO, USA) was added for 2 days to prevent excessive fibroblast contamination. SCs were purified via immunopanning<sup>33</sup> until > 90% purity of the neonatal SC cultures was achieved. To determine the purity of the SC culture according to our previous work<sup>25</sup>,  $5 \times 10^4$  cells were seeded into 24-well plates. Cells were immunostained with SC specific  $\alpha$ -S100 antibody (1:200, Z 0311, Dako, Denmark) in phosphate-buffered saline solution (PBS, Biochrom GmbH, Berlin, Germany)/0.3% Triton-X-100 (Roche Diagnostics GmbH, Germany)/5% bovine serum albumin (Sigma-Aldrich) and secondary Alexa 488-labeled goat  $\alpha$ -rabbit immunoglobulin G (IgG) antibody (1:500, A-11034, Thermo Fisher). As unspecific antibody, staining cytoplasm of both SCs and fibroblasts, we used mouse  $\alpha$ -Vimentin (1:1,000, V6630, Sigma-Aldrich) and secondary Alexa 555-labeled goat  $\alpha$ -mouse IgG antibody (1:500, A28180, Thermo Fisher). The nuclei of all cultured cells were stained with 4,6-diamidino-2-phenylindole (1:1000, Sigma-Aldrich). Fluorescent cells were visualized with an Olympus FX-70 fluorescence microscope. Photographs and overlays were taken on the same microscope using a digital image analysis system (cellSens Standard, Olympus, Germany).

After reaching this degree of purity, 2  $\mu$ M Forskolin (Thermo Fisher Scientific) were added to support SC proliferation. Passaged SCs at passages 8 to 10 were used as naïve control cells in the *in vitro* and *in vivo* studies as described in the following text.

### Nonviral Genetic Engineering of SCs

AMAXA nucleofection technique (Amamax device II; Lonza, Cologne, Germany) was used for the transfection of SCs. The plasmids, encoding for the low molecular weight

FGF-2 (pCAGGS-FGF-2<sup>18kDa</sup>-Flag; NCBI GenBank accession NM\_019305.2, 533–994 bp) were constructed as described previously<sup>34</sup>. For each transfection procedure,  $2.5 \times 10^6$  neonatal SCs at passages 8 to 10 were prepared by suspending them in 90  $\mu$ l basic transfection solution (basic glial cell nucleofection kit; Lonza). Then, 5  $\mu$ g of the plasmid DNA was added. For nucleofection AMAXA-specific cuvettes and the program T20 were used. Afterwards, the reaction was stopped by adding 900  $\mu$ l RPMI medium (Gibco, Darmstadt, Germany) enriched with 10% FCS (Gibco). SC survival was determined by using trypan blue staining (Sigma-Aldrich) and a Neubauer chamber system (Carl Roth & Co GmbH, Karlsruhe, Germany). The genetically engineered FGF2-SCs were further processed for the *in vitro* and *in vivo* experiments as described in the following text.

### Sodium Dodecyl Sulfate (SDS)–Polyacrylamide Gel Electrophoresis and Western Blot Analyses

Western blot analyses were performed according to our previous work<sup>21,25</sup> in order to detect endogenous FGF-2 expression as well as Flag-tagged FGF-2 expression in naïve as well as genetically engineered SCs (passages 9 to 11). The samples of transfected and nontransfected SCs were prepared in RIPA lysis buffer [137 mM NaCl (Thermo Fisher Scientific), 20 mM Tris-HCl (Sigma-Aldrich) pH 7, 525 mM  $\beta$ -glycerolphosphate (Sigma-Aldrich), 2 mM EDTA (Sigma-Aldrich), 1 mM sodium orthovanadate (Sigma-Aldrich), 1% sodium desoxycholate (Sigma-Aldrich), and 1% Triton-X-100 (Sigma-Aldrich)] containing phosphatase inhibitor (Roche) and protease inhibitor (Roche). Sonification was performed for 15 min and protein concentration was determined using bicinchoninic acid assay (Thermo Fisher Scientific). For endogenous FGF-2 western blot, 30  $\mu$ g of total protein lysates and for FGF-2<sup>18kDa</sup>-Flag western blot, 10  $\mu$ g of total protein lysates were dissolved in 1 $\times$  Laemmli buffer 1970 (5 $\times$ , 0.25 M Tris-HCl pH 8.0, 25% glycerol, 7.5% SDS, 0.25 mg/ml bromphenol blue, 12.5% v/v 2-mercaptoethanol; all Sigma-Aldrich). Protein separation was performed using a 15% gel in SDS–polyacrylamide gel electrophoresis. Separated proteins were blotted to a nitrocellulose membrane (RPN68D; Amersham Bioscience, Freiburg, Germany) by electrophoresis<sup>35</sup>. Endogenous FGF-2 and FGF-2<sup>18kDa</sup>-Flag were detected in the electrochemiluminescence system (Intas Science Imaging, Göttingen, Germany) using rabbit anti-FGF-2 (1:750, SC-79; Santa Cruz Biotechnology, Heidelberg, Germany) as primary antibody and secondary  $\alpha$ -rabbit horseradish peroxidase (HRP)-coupled antibody (1:4,000, Amersham NA934 V, GE Healthcare) or anti-Flag (1:1,000, F18-04; Sigma-Aldrich) as primary antibody and secondary  $\alpha$ -mouse HRP-coupled antibody [1:4,000, Amersham NA931, GE Healthcare, (Th, Greiner), Hamburg, Germany]. The signals were visualized with a chemiluminescent substrate solution (Pierce<sup>TM</sup>, Thermo Fisher Scientific).

### Preparation of 0.2% HA and 0.2% HAL

A synthetic laminin peptide consisting of 16 amino acids (containing 2 sequences of 2 pentapeptides found in laminin; synthesized at Bachem, Switzerland) and shown to guide neuronal migration, differentiation, regeneration, and survival was diluted with 1 ml of double distilled water in sterile conditions and filtered through a 0.45  $\mu$ m filter paper. Then, 1 ml of sterile solution of human recombinant superoxide dismutase 1 (SOD1; PRO-286, ProSpec, Israel) was added to the solution. Finally, 2 ml syringes containing 1% highly purified, high-molecular-weight (2.4 to 3.6 million Da) HA (EUFLEXXA<sup>®</sup>, Ferring Pharmaceuticals-Bio-Technology General Ltd., Israel) were diluted with PBS and added to the solution, to prepare a HA concentration of 0.4%. Pure HA was provided for control experiments in a concentration of 1% in PBS. The HAL as well as the pure HA were prepared in Israel and afterwards shipped to Germany. The HAL was kept at 4°C until use, including during shipment. Prior to in vivo or in vitro use, 1% HA was mixed with PBS to a concentration of 0.4% HA and then this was mixed 1:1 with serum-free N-2 medium to a concentration of 0.2% HA. According to the procedure, as described earlier for HA, 0.4% HAL was mixed 1:1 with serum-free N-2 medium to a concentration of 0.2% HAL prior to further use.

### Real-Time Quantitative Reverse Transcription Polymerase Chain Reaction (Real-time qRT-PCR)

Naïve as well as FGF2-SCs (see sections “Primary (Naïve) Neonatal Rat SCs” and “Nonviral Genetic Engineering of SCs”) at passages 10 to 12 were cultured within culture medium (see section “Primary (Naïve) Neonatal Rat SCs”) serving as positive control or within 0.2% of HA or 0.2% of HAL (see section “Preparation of 0.2% HA and 0.2% HAL”). For each condition, 350,000 cells per well were seeded into 2 poly-l-lysine (PLL)-coated wells of a 6-well plate (Nunc, Thermo Fisher Scientific). For PLL coating, the bottom of the culture flasks was covered with PLL for 30 min at 37°C. After removing the PLL flasks were washed 2 times with Ampuwa<sup>®</sup> (Fresenius Kabi, Bad Homburg, Germany). After 3 days in vitro, the supernatant was removed and cells were lysed and homogenized and total RNA was extracted according to the manufacturer’s protocol (RNeasy Plus Mini Kit, Qiagen, Hilden, Germany). For harvesting an appropriate amount of RNA, three different culture trials were needed for FGF2-SCs, while five culture trials were needed for SCs.

The RNA was eluted in 15  $\mu$ l of RNase free water (Qiagen) and completely used for cDNA synthesis with the iScript Kit (BioRad, Hercules, CA, USA). For qRT-PCR the following primer sequences were used: FGF-2-F: 5'-GAACCGGTACCTGGCTATGA-3'; FGF-2-R: 5'-CCA GGCGTTCAAAGAAGAAA-3'; brain-derived neurotrophic factor (BDNF)-F: 5'-GGACATATCCATGACCAGAAA GAA-3'; BDNF-R: 5'-GCAACAACCACAACATTATC

GAG-3'; glial cell-derived neurotrophic factor (GDNF)-F: 5'-CCAGAGAATTCCAGAGGGAAAGGT-3'; GDNF-R: 5'-TCAGTTCCTCCTTGGTTTCGTAGC-3'; nerve growth factor (NGF)-F: 5'-ACCTCTTCGGACACTCTGGA-3'; NGF-R: 5'-GTCCGTGGCTGTGGTCTTAT-3'.

Quantitative RT-PCR was performed according to Rumpel et al.<sup>36</sup> with Power SYBR-Green PCR Master Mix (Applied Biosystems, Foster City, CA, USA) on a StepOnePlus instrument (Applied Biosystems). Calculation of fold changes in cDNA levels was performed by using the 2(- $\Delta\Delta$ Ct) method and normalized to the housekeeping gene peptidylprolyl isomerase A (Ppia)-F: 5'-TGTGCCAG GGTGGTGA CTT-3'; Ppia-R: 5'-TCAAATTTCTCTCCG TAGATGGACTT-3'. The amount of cDNA achieved was sufficient for pooling cDNA for  $n = 3$  independent qRT-PCR runs per cell type and culture condition. For naïve SC cultured in HAL, however, the low proliferation as well as low cell density upon cell harvest (Figure 5) led to an amount of cDNA, which was only sufficient for pooling cDNA for  $n = 2$  independent analyses.

### In Vitro Analysis of Immunocompatibility Between Recipient Spleen (Spl) and Lymph Node (LN) Cells and Donor SCs via [<sup>3</sup>H]thymidine Incorporation Assay

Since sufficient numbers of neonatal rat SCs for this study were not obtainable from Lewis LEW/OrlRj breeds in reasonable time (small litter sizes and low proliferation rate of primary cells), we decided to use neonatal SCs from Wistar RjHan:WI breeds. The transfer of genetically modified SCs derived from Wistar RjHan:WI rats within CNGs into the recipient LEW/OrlRj rats displays, however, an allogenic transplantation, which comprises the risk of an immunoreaction and transplant rejection.

With the supplementary material to this study, we provide data on our evaluation of the probability for an immunoreaction to occur. Briefly, we performed in vitro proliferation assays of recipient Lewis LEW/OrlRj rat lymphocytes, derived from either the Spl or the cervical LN, cultivated with either donor Lewis LEW/OrlRj rat (Lew) SCs, serving as negative control, Wistar RjHan:WI rat (Wi) SCs, serving as experimental group, and Sprague Dawley RjHan:SD rat (SprD) SCs, serving as additional experimental group. And with this we could demonstrate that the probability to induce a host-versus-graft response with transplanting RjHan:WI-derived cells into LEW/OrlRj rats is close to zero (supplemental Figure S1).

### Manufacturing of Classic CNGs and CNG[F]s

Certified medical grade chitosan was derived from *Pandalus borealis* shrimp shells (Altakitin S.A., Lisboa, Portugal). CNGs were produced with an inner diameter of 2.1 mm and a length of 19 mm as described before<sup>21,22,37</sup> at Medovent GmbH (Mainz, Germany). All manufacturing steps were carried out under ISO 13485 requirements and

specifications. For the production of the chitosan films (CFs), 0.54 g medical grade chitosan (Medovent GmbH) was mixed with 35.78 ml of 0.5% acetic acid. After stirring the chitosan solution for 30 min, it was poured in a glass petri dish and dried for 3 to 4 days under the hood. The films were fixated with 68.8 ml 93.5% methanol and 3.9 ml 25% ammonia for 2 h. After removing the fixation solution, films were dried overnight and underwent UV sterilization on the following day. Then, they were cut into rectangular pieces with 15 mm length and 5 mm width. CFs were longitudinally z-folded and processed according to our previous publication<sup>21</sup>. Briefly, their middle line was perforated with a sharp needle, creating six holes with 2 mm distance to each other. After inserting the CFs concentrically into the chitosan tubes, the final CNG[F]s were sterilized by beta irradiation (11 kGy, 10 MeV) by BGS Beta-Gamma-Service GmbH & Co. KG (Wiehl, Germany)<sup>38</sup>. To rinse all CNGs and CNG[F]s for 20 min before they were implanted, 0.9% sodium chloride solution (NaCl 0.9%, B. Braun Melsungen AG, Melsungen, Germany) was used.

### Preparation of Genetically Engineered FGF2-SCs and Naïve SCs for Transplantation Within Composite Chitosan Nerve Grafts

Three days before surgical procedure neonatal rat SCs were genetically modified via nonviral transfection as described earlier (see section “Nonviral Genetic Engineering of SCs”). After transfection FGF2-SCs were seeded into PLL-coated culture flasks (Nunc, Thermo Fisher Scientific) for 24 h to recover from transfection. Then, culture medium was changed to serum-free N-2 medium again for 24 h. For comparability, nontransfected cells were collected from their flasks, reseeded and cultured for 24 h under serum-free conditions as well.

At the day of nerve reconstruction surgery, either  $1 \times 10^6$  FGF2-SCs or naïve SCs were mixed with 70  $\mu$ l 0.2% HAL and kept on ice until filled into tubular nerve grafts (see section “Experimental Design”).

To determine the protein expression of either naïve or FGF2-SCs, at the time of nerve graft preparation, sister batches of  $1 \times 10^6$  detached naïve/FGF2-SC were collected, centrifuged, and their pellets washed with PBS (Biochrom GmbH, Berlin, Germany). After another step of centrifugation, the pellets were stored at  $-80^\circ\text{C}$  for western blot analysis (see section “SDS–Polyacrylamide Gel Electrophoresis and Western Blot Analyses”).

### Experimental Design

The differently composed bioartificial nerve grafts were comprehensively evaluated during an observation period of 120 days. Due to logistic limitations the whole in vivo experiment was divided into two consecutive parts that followed an identical schedule but allowed to handle and observe smaller groups at a time (Table 1).

**Table 1.** Experimental Design.

Group	First surgery	Second surgery	Total
ANG	$n = 4$	$n = 2$	$n = 6$
CNG+HA	/	$n = 5$	$n = 5$
CNG+HAL	$n = 4$	$n = 4$	$n = 8$
CNG+HAL+SC	$n = 4$	$n = 4$	$n = 8$
CNG+HAL+FGF2-SC	$n = 4$	$n = 4$	$n = 8$
CNG[F]+HA	/	$n = 5$	$n = 5$
CNG[F]+HAL	$n = 4$	$n = 4$	$n = 8$
CNG[F]+HAL+SC	$n = 4$	$n = 4$	$n = 8$
CNG[F]+ HAL+FGF2-SC	$n = 4$	$n = 4$	$n = 8$

Summary of the experimental groups included into the in vivo experiment. The total experiment was divided into two parts. The table shows the respective numbers ( $n$ ) of reconstructed sciatic nerves per part-experiment (first surgery, second surgery) per experimental group (left column) as well as total numbers of reconstructed sciatic nerves per experimental group ( $n$ , right column).

ANG: autologous nerve graft; FGF-2: fibroblast growth factor 2; HA: hyaluronic acid; HAL: hyaluronic acid–laminin hydrogel; SC: Schwann cell.

We did not include groups receiving only empty CNGs or CNG[F]s, because these grafts have been evaluated by us before in the same comprehensive animal model (critical sciatic nerve defect sizes)<sup>21,37</sup>. We did also not test nerve guides filled with SCs, only suspended in medium, since we also previously demonstrated that this attempt is not increasing the regeneration support already given by CNG[F]s and even might have had negatively interfered with the regeneration process<sup>21</sup>. Therefore, we could additionally reduce the number of animals subjected to the current study.

For functional evaluation (see section “Assessment of Functional Recovery”), electrodiagnostic measurements were performed 60, 90, and 120 days after reconstruction surgery. After the last final measurements, animals were killed and tissues for endpoint analyses were harvested (see sections “Muscle Weight Ratio” and “Nerve Histomorphometry”).

### Animals and Surgical Procedure

Animal experiments were conducted in accordance with the German animal protection law and with the European Communities Council Directive 2010/63/EU for the protection of animals used for experimental purposes. All experiments were approved by the Local Institutional Animal Care and Research Advisory and the animal care committee of Lower-Saxony, Germany (approval code: 33.12 42502-04-16/2320; approval date: 30.11.2016). Here, we used 64 adult female Lewis rats (LEW/OrlRj; average weight at the day of surgery:  $195.1 \pm 1.2$  g) obtained from Janvier Labs SAS [Genest Saint Isle (Le), France] at an age of 12 weeks. In groups of four animals, they were housed under standard conditions (room temperature  $22.2^\circ\text{C}$ ; humidity 55.5%; light/ dark cycle of 14 h/10 h). Food and water was provided ad libitum. Two weeks before surgery, until completion of the study, the rats were orally treated with amytriptiline hydrochloride

(13.5 mg/kg/day, Amitriptylin-neuraxpharm<sup>®</sup>, Neuraxpharm Arzneimittel GmbH, Langenfeld, Germany) by adding it to their drinking water in order to prevent events of automutilation<sup>39</sup>. The animals' health states were controlled every 2 to 3 days.

Surgical interventions as well as noninvasive electrodiagnostic recordings were carried out under aseptic conditions including adequate anesthesia and analgesia. For deep anesthesia, chloral hydrate (370 mg/kg, Sigma-Aldrich) was injected intraperitoneally. During anesthesia, the animals were placed on a heating pad and their rectal body temperature regularly controlled not to fall below 36.5°C.

At 5 min prior to nerve transection, a local topical application of bupivacaine (0.25%, Carbostesin<sup>®</sup>, AstraZeneca GmbH, Wedel, Germany) and lidocaine (2%, Xylocain<sup>®</sup>, AstraZeneca GmbH) on the sciatic nerves was performed to ensure sufficient analgesia. In addition to that, butorphanol (0.5 mg/kg, Torbugesic<sup>®</sup>, Pfizer, New York City, NY, USA) was injected subcutaneously at the day of surgery, the following 2 days and before electrodiagnostic recordings.

In accordance to studies, previously carried out by our group<sup>18,21,25</sup>, the left sciatic nerve was exposed at mid-thigh level. The first nerve transection was performed 5 mm distal to the aponeurosis of the gluteus muscle by using a pair of micro scissors.

For reconstruction using ANGs, the second nerve transection was performed 15 mm further distal to the first transection site. After reversing and rotating it around by 180°, the nerve piece was sutured by three epineural 9-0 stitches each to the proximal and the distal nerve end.

For tubular nerve graft repair (groups listed in Table 1) the second nerve transection was performed 13 mm distal to the initial one and the nerve piece was removed.

Before filling the artificial nerve grafts with the corresponding cell-free or cell-carrying luminal filler (see section "Preparation of 0.2% HA and 0.2% HAL"), CNGs and CNG[F]s were stored in 0.9% sodium chloride rinsing solution (NaCl 0.9%, B. Braun Melsungen AG) for at least 20 min. The filling was performed immediately before suturing the respective nerve grafts into the nerve defect. Therefore 60 µl of the respective luminal filler (HA, HAL, HAL+SC, or HAL+FGF2-SC) were pipetted into the grafts' lumen. For filling CNG[F]s, 30 µl of filling volume was pipetted into either chamber of the nerve guides.

The appropriately prepared tubular nerve grafts were transferred into the nerve defect and sutured to the nerve ends with one epineural 9-0 stitch at each end. An overlap of 2 mm at each site was generated with a 15 mm sciatic nerve gap, bridged with the grafts.

Wounds were closed with three to four resorbable sutures of the femoral biceps muscle (3-0 Polysorb, UL-215, Covidien, Dublin, Ireland) followed by skin suture with three to four nonresorbable mattress sutures (4-0 Ethilon<sup>TM</sup>II, EH7791 H, Ethicon, Somerville, NJ, USA).

## Assessment of Functional Recovery

**Motor Recovery: Repeated Transcutaneous Electrodiagnostic Recordings.** Noninvasive electrodiagnostic recordings were performed at 60, 90, and 120 days after surgery as previously described by our group<sup>18</sup>. Briefly, deeply anesthetized animals were placed in prone position on a heating pad that was only switched off for the short period of actual recording to again keep their body temperature  $\geq 36.5^\circ\text{C}$ . Monopolar needle electrodes were inserted transcutaneously and the nerves were stimulated with the help of a Dantec<sup>®</sup> Keypoint<sup>®</sup> Focus device (Natus Europe GmbH, Planegg, Germany) by transmitting single electrical impulses (100 µs, 1 Hz). The stimulation intensity was gradually increased up to 30% supramaximal level. The reconstructed sciatic nerve was either stimulated proximal to the transplanted graft at the sciatic notch or distal to it in the popliteal fossa. Evoked compound muscle action potentials (CMAPs) were recorded from the tibialis anterior muscle (TA) and the plantar muscles (PL) at the reconstructed left side of the animals (experimental values) or the contralateral healthy right side (reference values). CMAP amplitude (baseline to negative peak of the M-wave) areas were calculated. Then functional axon loss was calculated as previously described<sup>40</sup>. CMAP amplitude areas, as well as axon losses, were calculated and included into statistical analyses for lesioned sides of all animals. In cases, when animals did not recover evocable CMAPs, the amplitude area was set to 0 and the axon loss to 100% for statistical analysis, respectively. Healthy baseline reference values for CMAP amplitude areas of the nonlesioned right hind limb were collected from those animals showing evocable CMAPs at 120 days post surgery in the TA or PL muscles of the lesioned left side. Accordingly, mean TA CMAP amplitude area was calculated from 27 animals, and the mean PL CMAP amplitude area was calculated from 15 animals (see Results: Repeated Transcutaneous Electrodiagnostic Recordings).

**Muscle Weight Ratio.** After completion of the observation period, animals were transferred into carbon dioxide atmosphere for inducing deep anesthesia and killed by cervical dislocation. Both lower limb muscles [TA and gastrocnemius (GC) muscle] were explanted from the lesioned left and healthy control right side. The muscles were weighed and muscle weight (g) of the lesioned side was divided by the muscle weight (g) of the healthy control side for calculation of muscle weight ratios (MWRs).

## Nerve Histomorphometry

In general, histomorphometry of the nerves was performed as described earlier<sup>35</sup>. The regenerated tissue within the lumen of the nerve guides including the central CF, for CNG[F]s, as well as segments of the distal nerve (5 mm in length in continuation of the nerve graft) were explanted for morphometrical analyses. Control tissue samples ( $n = 6$ )

were dissected in corresponding locations from contralateral healthy nerves.

Distal nerve segments were fixed in Karnovsky solution (2% PFA, 2.5% glutaraldehyde in 0.2 M sodium cacodylate buffer, pH 7.3) for 24 h<sup>40</sup>. Afterwards, the samples were transferred to 0.1 M sodium cacodylate buffer containing 7.5% sucrose and post-fixation was carried out in 1% osmium tetroxide for 1.5 h. For myelin sheaths staining, the samples were immersed in 1% potassium dichromate (for 24 h), 25% ethanol (for 24 h), and finally hematoxylin (0.5% in 70% ethanol, for 24 h). After Epon embedding, semi-thin cross-sections (1  $\mu$ m thickness) were prepared and toluidine blue staining was additionally performed to enhance myelin sheaths staining. Sections were mounted with Mowiol (Merck Millipore, MA, USA).

According to our previous work<sup>41</sup>, semi-thin nerve cross-sections were evaluated using a BX50 microscope (Olympus Europa SE & Co. KG, Hamburg, Germany), which was expanded with a prior controller (MBF Bioscience, Williston, VT, USA). Analyses were performed in two randomly selected sections by using the Stereo Investigator version 11.04 (MBF Bioscience). The cross-sectional area (in 20 $\times$  magnification), the total number of myelinated fibers (in 100 $\times$  magnification), and the nerve fiber density were analyzed with a two-dimensional procedure (optical fractionator; grid size: 150  $\times$  150  $\mu$ m<sup>2</sup>; counting frame size: 30  $\times$  30  $\mu$ m<sup>2</sup>; counting of "fiber tops" as suggested by colleagues)<sup>42</sup>. Samples from all animals were included into stereological evaluation. If there was no axonal recovery by the end of the study, the total number of myelinated fibers and the nerve fiber density (number of myelinated fibers/square mm) were set to 0 for statistical analysis.

For analysis of nerve morphometry, photomicrographs of four randomly selected areas of each cross section (in 100 $\times$  magnification) were taken for evaluation of axon and fiber diameters, myelin thicknesses, and *g*-ratios. Animals with no axonal regeneration after 120 days as determined in the stereological evaluation had to be excluded from this analysis resulting in  $\leq 3$  analyzed samples per group as follows: CNG+HA ( $n = 1$ ), CNG+HAL ( $n = 2$ ), CNG+HAL+SC ( $n = 0$ ), CNG[F]+HAL+SC ( $n = 2$ ), CNG+HAL+FGF2-SC ( $n = 1$ ), CNG[F]+HAL+FGF2-SC ( $n = 1$ ). For the analyses, *g*-ratio plug-in (<http://gratio.efil.de/>) in ImageJ version 1.48 (National Institutes of Health, Bethesda, MD, USA) was used. Ten axons per picture were included into evaluation, so that 80 axons per animal were evaluated in total. For calculation of axon and fiber diameters, we made the assumption that they are circularly shaped.

### Statistical Analyses

GraphPad Prism version 6.07 (GraphPad Software, San Diego, CA, USA) was used to perform statistical analyses of the data, recorded in this study. To detect significant differences, one-way analysis of variance (ANOVA) followed by Dunnett's multiple comparisons (real-time qRT-PCR),

two-way ANOVA followed by Tukey's multiple comparisons (electrodiagnostic measurements), or Kruskal–Wallis test followed by Dunn's multiple comparisons (MWRs, histomorphometrical analyses) were applied. The *P*-value for statistical significance was set at  $P < 0.05$ . All results are presented as median  $\pm$  range, percentages, mean  $\pm$  SEM, mean  $\pm$  SD, or single values (in cases of  $n = 1$  or  $n = 2$ ) as indicated in the respective tables or figures. For the statistical analyses of electrodiagnostic measurements (CMAP amplitude area, axon loss) all animals were included. For those animals, which did not show evocable CMAPs, values for CMAP amplitude area were set to 0 and values for axon loss were set to 100. For the statistical analyses of histomorphometrical analyses (axon diameter, fiber diameter, *g*-ratio, myelin thickness), those animals, which showed no regenerated axons in the distal stump (total number of myelinated fibers = 0; nerve fiber density = 0 axons/mm<sup>2</sup>), had to be excluded from further morphometrical analyses.

## Results

### SDS–Polyacrylamide Gel Electrophoresis and Western Blot Analyses

For evaluation of protein level expression of naïve as well as FGF2-SCs, western blot analyses were performed 48 h after regular culture or transfection (Figure 1). Endogenous strong expression of two FGF-2 isoforms (18 kDa, 23 kDa) could be detected in FGF2-SCs (Figure 1A). In naïve SCs we detected all three isoforms of FGF-2 (18 kDa, 21 kDa, 23 kDa). FGF-2<sup>18 kDa</sup> revealed a strong signal, while FGF-2<sup>21 kDa</sup> and FGF-2<sup>23 kDa</sup> were expressed at a lower level (Figure 1B). Successful overexpression of FGF-2<sup>18kDa</sup>-Flag was proven by showing strong bands in western blot analyses from cell lysates obtained from FGF2-SCs used in either of the two consecutive *in vivo* experiments (Figure 1C). Application of protein extract from nontransfected naïve SCs did not result in any detectable band (Figure 1C).

### Repeated Transcutaneous Electrodiagnostic Recordings

Functional motor recovery was assessed by applying noninvasive electrodiagnostic recordings, which were periodically performed every 30 days from 60 days post surgery onwards. CMAPs of the anterior tibial muscle (TA; see Table 2) and of the PL (see Table 3) were recorded for calculating CMAP amplitude areas as well as axon loss. Healthy baseline reference values were derived from the right uninjured paw of animals with evocable CMAPs on the lesioned site (healthy mean: TA: 45.81  $\pm$  3.12 ms \* mV,  $n = 27$ ; PL: 1.601  $\pm$  0.392 ms \* mV,  $n = 15$ , see section "Motor Recovery: Repeated Transcutaneous Electrodiagnostic Recordings" for details on calculation).

Table 2 lists the results from CMAP recordings from the TA muscle as described in detail as follows.

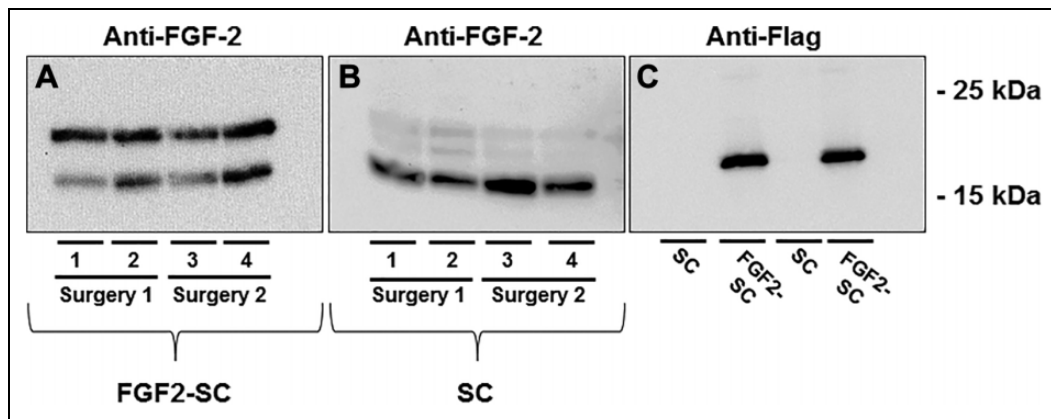


**Fig 1.** Results of western blot analyses of cell lysates from naive or genetically engineered Schwann cells. Detection of endogenous fibroblast growth factor 2 (FGF-2) expression (A and B) and Flag-tagged FGF-2<sup>18kDa</sup> overexpression (C) and by western blotting of cell lysates derived from naive Schwann cells (SCs) and genetically engineered FGF-2-overexpressing Schwann cells (FGF2-SCs) cultured for 24 h in specific SC medium and another 24 h in serum-free N2 medium. Endogenous FGF-2<sup>18 kDa</sup> and FGF-2<sup>23 kDa</sup> were detected in lysates of FGF2-SCs, showing a strong signal for both isoforms. In naive SCs all isoforms of FGF-2 (18 kDa, 21 kDa, and 23 kDa) were detected with a strong signal only detected for FGF-2<sup>18 kDa</sup>. FGF-2<sup>18kDa</sup>-Flag was detected in lysates derived from FGF2-SCs, while lysates of naive SCs did not result in any detection. Each  $n = 4$  (indicated by columns 1 to 4).

**Table 2.** CMAP Recordings from the TA Muscle Displaying Motor Recovery.

	Group	Animals per group	CMAP amplitude area (ms * mV)	Axon loss (%)
60 days post surgery	ANG	6/6 (100%)	16.94 ± 4.15	55.94 ± 8.42
	CNG+HA	0/5 (0%)	0.00 ± 0.00	100 ± 0.00
	CNG+HAL	2/8 (25%)	3.64 ± 2.63	90.02 ± 7.76
	CNG+HAL+SC	0/8 (0%)	0.00 ± 0.00	100 ± 0.00
	CNG+HAL+FGF2-SC	0/8 (0%)	0.00 ± 0.00	100 ± 0.00
	CNG[F]+HA	0/5 (0%)	0.00 ± 0.00	100 ± 0.00
	CNG[F]+HAL	1/8 (12.5%)	0.00 ± 0.00	100 ± 0.00
	CNG[F]+HAL+SC	0/8 (0%)	0.00 ± 0.00	100 ± 0.00
	CNG[F]+HAL+FGF2-SC	0/8 (0%)	0.00 ± 0.00	100 ± 0.00
90 days post surgery	ANG	6/6 (100%)	32.62 ± 4.03	-0.93 ± 9.20*
	CNG+HA	0/5 (0%)	0.00 ± 0.00####	100 ± 0.00####
	CNG+HAL	2/8 (25%)	7.60 ± 5.54###	75.53 ± 18.78###
	CNG+HAL+SC	0/8 (0%)	0.00 ± 0.00####	100 ± 0.00####
	CNG+HAL+FGF2-SC	0/8 (0%)	0.00 ± 0.00####	100 ± 0.00####
	CNG[F]+HA	4/5 (80%)	9.93 ± 3.21	73.98 ± 8.40###
	CNG[F]+HAL	2/8 (25%)	9.21 ± 3.18###	71.48 ± 10.80####
	CNG[F]+HAL+SC	2/7 (28.6%)	7.07 ± 4.68###	77.93 ± 15.25####
	CNG[F]+HAL+FGF2-SC	1/8 (12.5%)	9.93 ± 3.21####	92.85 ± 7.15####
120 days post surgery	ANG	6/6 (100%)	46.19 ± 4.53***	-1.22 ± 9.16*
	CNG+HA	1/5 (20%)	4.70 ± 4.70####	89.93 ± 10.07####
	CNG+HAL	2/8 (25%)	12.81 ± 8.45####	71.96 ± 18.55####
	CNG+HAL+SC	0/8 (0%)	0.00 ± 0.00####,\$	100 ± 0.00####
	CNG+HAL+FGF2-SC	0/8 (0%)	0.00 ± 0.00####,\$	100 ± 0.00####
	CNG[F]+HA	4/5 (80%)	23.84 ± 6.24	48.89 ± 13.38
	CNG[F]+HAL	7/8 (87.5%)	16.84 ± 6.39####	61.75 ± 10.08###
	CNG[F]+HAL+SC	3/7 (42.9%)	17.72 ± 8.99####	60.94 ± 19.90###
	CNG[F]+HAL+FGF2-SC	3/8 (37.5%)	23.84 ± 6.24####	90.80 ± 10.07####

Recovery rates (second column), total numbers (percentage), CMAP amplitude areas (third column), and axon losses (fourth column) were derived from noninvasive electrodiagnostic recordings from the TA muscle 60, 90, and 120 days after reconstruction.

Column 2: numbers of animals displaying evocable CMAPs are shown as numbers/total number of animals in the group; in brackets the related percentage is indicated.

Column 3 and 4: Significant differences ( $P < 0.05$ ) were detected by two-way analysis of variance, followed by Tukey's multiple comparisons ( $*P < 0.05$ ,  $***P < 0.001$  vs. ANG 60 days;  $###P < 0.01$ ,  $####P < 0.001$  vs. ANG at the same time point;  $\$P < 0.05$  vs. CNG[F] + HA). Results are presented as mean ± SEM.

ANG: autologous nerve graft; CMAP: compound muscle action potential; CNG: chitosan-based nerve graft; FGF-2: fibroblast growth factor 2; HA: hyaluronic acid; HAL: hyaluronic acid-laminin hydrogel; SC: Schwann cell; TA: tibialis anterior.



**Table 3.** CMAP Recordings from the PL Muscles Displaying Motor Recovery.

	Group	Animals per group	CMAP amplitude area (ms * mV)	Axon loss (%)
60 days post surgery	ANG	5/6 (83.3%)	0.25 ± 0.16	88.92 ± 4.40
	CNG+HA	0/5 (0%)	0.00 ± 0.00	100 ± 0.00
	CNG+HAL	0/8 (0%)	0.00 ± 0.00	100 ± 0.00
	CNG+HAL +SC	0/8 (0%)	0.00 ± 0.00	100 ± 0.00
	CNG+HAL+FGF2-SC	0/8 (0%)	0.00 ± 0.00	100 ± 0.00
	CNG[F]+HA	0/5 (0%)	0.00 ± 0.00	100 ± 0.00
	CNG[F]+HAL	0/8 (0%)	0.00 ± 0.00	100 ± 0.00
	CNG[F]+HAL+SC	0/8 (0%)	0.00 ± 0.00	100 ± 0.00
	CNG[F]+HAL+FGF2-SC	0/8 (0%)	0.00 ± 0.00	100 ± 0.00
90 days post surgery	ANG	6/6 (100%)	1.62 ± 0.72***	23.76 ± 30.65
	CNG+HA	0/5 (0%)	0.00 ± 0.00####	100 ± 0.00#
	CNG+HAL	1/8 (12.5%)	0.21 ± 0.21####	88.80 ± 11.20#
	CNG+HAL +SC	0/8 (0%)	0.00 ± 0.00####	100 ± 0.00###
	CNG+HAL+FGF2-SC	0/8 (0%)	0.00 ± 0.00####	100 ± 0.00###
	CNG[F]+HA	0/5 (0%)	0.00 ± 0.00####	100 ± 0.00#
	CNG[F]+HAL	2/8 (25%)	0.03 ± 0.02####	100 ± 0.00##
	CNG[F]+HAL+SC	1/7 (14.3%)	0.11 ± 0.11####	94.24 ± 5.76#
	CNG[F]+HAL+FGF2-SC	0/8 (0%)	0.00 ± 0.00####	100 ± 0.00###
120 days post surgery	ANG	6/6 (100%)	1.37 ± 0.32*	-1.21 ± 30.34***
	CNG+HA	0/5 (0%)	0.00 ± 0.00####	100 ± 0.00####
	CNG+HAL	2/8 (25%)	0.42 ± 0.28#	69.54 ± 23.20###
	CNG+HAL +SC	0/8 (0%)	0.00 ± 0.00####	100 ± 0.00####
	CNG+HAL+FGF2-SC	0/8 (0%)	0.00 ± 0.00####	100 ± 0.00####
	CNG[F]+HA	2/5 (40%)	0.18 ± 0.12#	91.54 ± 5.66####
	CNG[F]+HAL	2/8 (25%)	0.23 ± 0.19###	91.54 ± 5.66####
	CNG[F]+HAL+SC	2/7 (28.6%)	0.45 ± 0.38	62.68 ± 34.04#
	CNG[F]+HAL+FGF2-SC	0/8 (0%)	0.00 ± 0.00####	100 ± 0.00####

Recovery rates (second column), total numbers (percentage), CMAP amplitude areas (third column), and axon losses (fourth column) were derived from noninvasive electrodiagnostic recordings from the plantar (PL) muscles 60, 90, and 120 days after reconstruction. Column 2: numbers of animals displaying evocable CMAPs are shown as numbers/total number of animals in the group, in brackets the related percentage is indicated.

Columns 3 and 4: Significant differences ( $P < 0.05$ ) were detected by two-way analysis of variance, followed by Tukey's multiple comparisons (\* $P < 0.05$ , \*\*\* $P < 0.001$  vs. ANG 60 days; # $P < 0.05$ , ## $P < 0.01$ , ### $P < 0.001$  vs. ANG at the same time point). Results are presented as mean ± SEM.

ANG: autologous nerve graft; CMAP: compound muscle action potential; CNG: chitosan-based nerve graft; FGF-2: fibroblast growth factor 2; HA: hyaluronic acid; HAL: hyaluronic acid-laminin hydrogel; PL: plantar muscles; SC: Schwann cell.

Successful reinnervation of the TA muscle was fastest and most complete in the ANG-treated animals, which demonstrated 100% recovery rate (percentage of animals per group, demonstrating evocable CMAPs) already 60 days post-surgery. At this time point, also the first animals of the CNG+HAL (25%) and the CNG[F]+HAL (12.5%) group showed evocable CMAPs. No signs of motor recovery were found in the other artificial nerve guide groups.

Ninety days post surgery the rate of functional motor recovery as observed in the ANG (100%) and CNG+HAL (25%) groups was not changed, while it did increase in the CNG[F]+HAL group to 25%. Interestingly, another cell-free transplantation condition, CNG[F]+HA, demonstrated 80% TA motor recovery rate at this time. Reconstruction of the nerve defects and additional cell transplantation did result in low recovery rates, such as 28.6% in the CNG[F]+HAL+SC group and 12.5% in CNG[F]+HAL+FGF2-SC-treated animals. It is noteworthy that the cell-transplantation approach using hollow nerve guides, as well as adding HA alone into hollow nerve guides, did not result in detectable motor

recovery (0% recovery rate in the CNG+HAL+SC, CNG+HAL+FGF2-SC, and CNG+HA groups).

After 120 days still none of the artificial nerve guide groups revealed complete functional motor recovery. The recovery rate in the CNG+HAL group was still 25% (not improved over time), while the CNG-HA group did finally include one animal, representing 20% TA recovery rate. The highest recovery rates among the artificial nerve guide groups were achieved by the CNG[F]+HA (80%, not changed to 90 days post-surgery) and the CNG[F]+HAL (87.5%, increased from 90 days post surgery) groups. Groups transplanted with cell-carrying HAL in two-chambered nerve guides showed a further increase of their recovery rates up to 42.9% in the CNG[F]+HAL+SC group and 37.5% in the CNG[F]+HAL+FGF2-SC group. The cell-transplantation approach, using hollow nerve guides, still did not result in detectable motor recovery (0% for CNG+HAL+SC and CNG+HAL+FGF2-SC groups).

Considering the TA-CMAP amplitude area, which can be directly correlated to the amount of functional axons

(Table 2, third column) reinnervating the target tissue, ANG-treated animals performed significantly better from 90 days post-surgery onwards when compared to the artificial nerve guide groups at the same time point, and reached healthy baseline reference values at 120 days post-surgery.

At 120 days post-surgery, the mean amplitude in the CNG[F]+HA group was still about one third of that of ANG-treated animals; statistical analysis did, however, not reveal significant difference to the ANG group anymore, while showing a significantly larger TA-CMAP amplitude area in comparison to the CNG+HAL+SC and CNG+HAL+FGF2-SC groups (indicated by \$ in Table 2).

With regard to the calculated loss of functional axons (right column “axon loss” in Table 2), ANG-treated animals significantly improved from 90 days onwards, revealing a significantly lower axon loss when compared to the artificial nerve guide groups at that time point. At 120 days, only the CNG[F]+HA group revealed no significant differences when compared to ANG-treated animals, while animals of all other artificial nerve guide groups showed a significantly higher axon loss when compared to the gold standard.

Table 3 lists the results from CMAP recordings from the PL muscles, which are located more distal than the TA muscle, and even lower recovery rates have been recorded for this target area of the reconstructed sciatic nerves. Overall, the best conditions already detected in electrodiagnostic analysis of motor recovery of the TA muscle did also support PL muscle reinnervation as described in detail in the following text. ANG application was superior to all other groups, reaching a recovery rate of 100% at 90 days after reconstruction surgery. First, animals of the CNG+HAL (12.5%), CNG[F]+HAL (25%), and CNG[F]+HAL+SC (14.3%) groups showed reinnervation of the PL muscles at 90 days post surgery. After 120 days post-surgery, the CNG[F]+HA group additionally revealed animals with evocable CMAPs (40%). However, animals of the CNG+HA, CNG+HAL+SC, CNG+HAL+FGF2-SC, and CNG[F]+HAL+FGF2-SC groups remained without any signs of functional motor recovery in the PL muscles.

Looking at the PL-CMAP amplitude area (Table 3, third column), ANG-treated animals performed significantly better when compared to the artificial nerve guide groups from 90 days onwards, reaching healthy baseline reference values at this time point (CMAP amplitude area:  $1.601 \pm 0.392$  ms \* mV).

Similar results apply to the calculation of axon loss (Table 3, right column), with ANG-treated animals achieving a significantly lower axon loss from 90 days post-surgery onwards when compared to all other artificial nerve guide groups.

### Motor Recovery: MWRs

After finishing the observation period of 120 days, animals were killed and the two biggest muscles from the lower limb, the TA muscle as well as the GC muscle, were harvested.

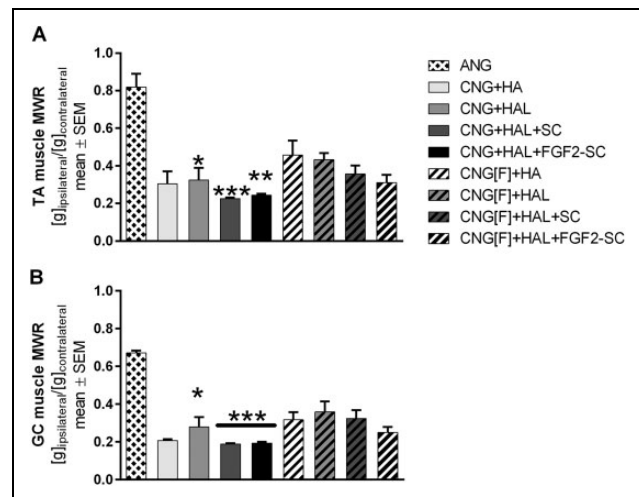


**Fig 2.** Bar graphs depicting the muscle weight ratios (MWRs) of tibialis anterior (A, TA muscle) and gastrocnemius (B, GC muscle) muscles at 120 days after reconstruction surgery. Kruskal–Wallis test with Dunn’s multiple comparisons were applied to detect significant differences (\* $P < 0.05$ , \*\* $P < 0.01$ , \*\*\* $P < 0.001$  vs. autologous nerve graft [ANG]). Results are presented as mean  $\pm$  SEM.

MWRs between the treated and healthy hind limb were calculated in order to determine the degree of successful target reinnervation in addition to the electrodiagnostic measurements.

As depicted in Figure 2, similar results for MWRs of TA (Figure 2A) and GC (Figure 2B) muscles were obtained. The highest MWRs were achieved by the ANG group, revealing significantly higher MWRs when compared to the CNG+HAL, CNG+HAL+SC, and CNG+HAL+FGF2-SC groups.

Among the artificial nerve guide groups, highest MWRs were obtained by the CNG[F]+HA (TA muscle) and the CNG[F]+HAL (GC muscle) groups. No significant differences could be detected, however, when comparing the animals that have been treated with artificial nerve guides among each other.

### Macroscopic Evaluation of the Regenerated Tissue Within the Nerve Grafts

Upon harvest of distal nerve tissue for histomorphometrical analysis at 120 days post surgery, we macroscopically examined if tissue regenerated through the nerve grafts (Figure 3) and finally connected the proximal and the distal nerve ends again. As summarized in Table 4, we categorized the degree of regeneration related to the visible appearance of the regenerated tissue. Category 1, substantial/two cables (Table 4, second column), refers to the event that either a single-stranded tissue connection of  $\geq 0.5$  mm in diameter or a two-stranded tissue connection was formed between the former nerve ends. The second event was only possible if CNG[F]s were used. Also implanted ANGs were included in

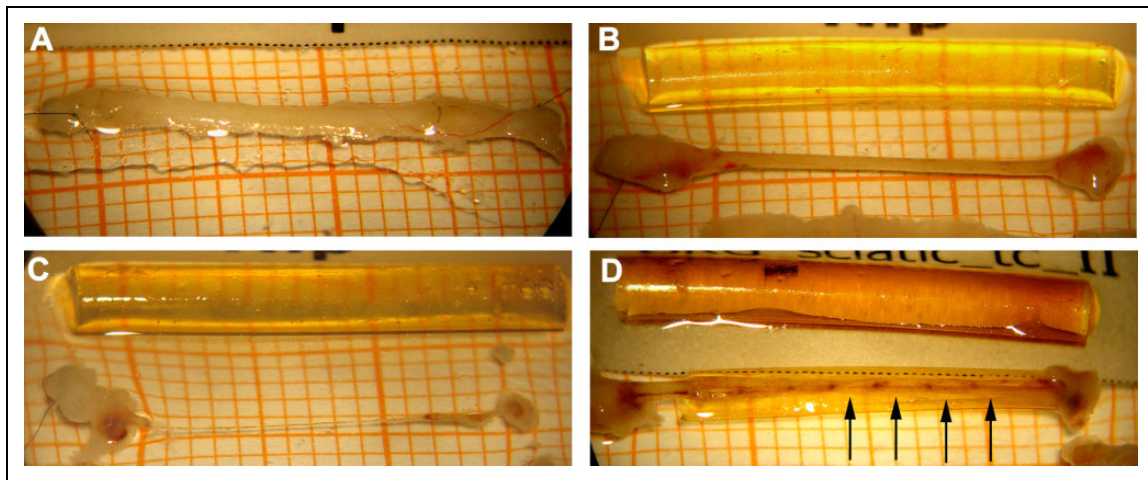


**Fig 3.** Macroscopical appearance of the regenerated tissue between the proximal and the distal nerve end upon tissue harvest 120 days after reconstruction. (A) Macroscopic appearance of an autologous nerve graft (ANG), this registered in category 1 = substantial tissue regeneration. (B) Another example for category 1 regeneration, here from the CNG+HAL group. (C) An example of category 3 tissue regeneration, a hair thin connection between the two nerve ends, here from the CNG+HAL+FGF2-SC group. (D) Tissue regeneration through two-chambered CNG[F]s in some cases resulted in the formation of two tissue cables also registered in category 1. The example is derived from the CNG[F]+HAL group and additionally demonstrates vascularized tissue bridges that have grown through the perforations in the chitosan film (arrows).

**Table 4.** Characterization of Regenerated Tissue Within the Grafts 120 Days Post Surgery.

Group	Category 1: Substantial/2 cables	Category 2: Thin	Category 3: Very thin	Category 4: No regenerated tissue
ANG	6/6 (100%)	0/8 (0%)	0/8 (0%)	0/8 (0%)
CNG+HA	1/5 (20%)	2/5 (40%)	0/8 (0%)	2/5 (40%)
CNG+HAL	2/8 (25%)	0/8 (0%)	5/8 (62.5%)	1/8 (12.5%)
CNG+HAL +SC	0/8 (0%)	3/8 (37.5%)	4/8 (50%)	1/8 (12.5%)
CNG+HAL+FGF2-SC	0/8 (0%)	0/8 (0%)	2/8 (25%)	6/8 (75%)
CNG[F]+HA	4/5 (80%)	1/5 (20%)	0/8 (0%)	0/8 (0%)
CNG[F]+HAL	7/8 (87.5%)	0/8 (0%)	0/8 (0%)	1/8 (12.5%)
CNG[F]+HAL+SC	3/7 (42.9%)	2/7 (28.6%)	2/7 (28.6%)	0/8 (0%)
CNG[F]+HAL+FGF2-SC	3/8 (37.5%)	5/8 (62.5%)	0/8 (0%)	0/8 (0%)

Contents of regrown tissue within the nerve grafts were examined macroscopically and categorized into formation of substantial tissue/two tissue cables (second column, category 1), thin (third column, category 2), very thin (fourth column, category 3), and no regenerated tissue (fifth column, category 5). Numbers of animals displaying tissue recovery within a respective category are shown as numbers/total number of animals in the group; in brackets the related percentage is indicated.

ANG: autologous nerve graft; CNG: chitosan-based nerve graft; FGF-2: fibroblast growth factor 2; HA: hyaluronic acid; HAL: hyaluronic acid–laminin hydrogel; SC: Schwann cell.

this category. Category 2, thin (Table 4, third column), refers to the event that in either graft type a single-stranded tissue connection of  $\leq 0.5$  mm in diameter was formed. Category 3, very thin (Table 4, fourth column), refers to the event that in either graft type a single-stranded tissue connection was formed that was not much thicker than a hair. Finally, in category 4, no regenerated tissue (Table 4, right column), the nerve gap was not bridged by any visible tissue.

In cases of ANG-treated animals, category 1 regeneration was found in 100% of the rats. In the CNG+HA group, 60% of the animals showed regenerated tissue of category 1 (one animal) or 2 (two animals), while 40% did not reveal any regeneration (category 4). Only one (12.5%) of the

CNG+HAL-treated animals remained without any visible regeneration (category 4). However, most of the animals (62.5%) only revealed a very thin tissue connection between the nerve ends (five animals, category 3), while two animals showed a category 1 regeneration. In contrast to the CNG+HAL group, there were no animals in the CNG+HAL+SC and the CNG+HAL+FGF2-SC groups showing substantial tissue regeneration (category 1). Seventy five percent of the animals in the CNG+HAL+FGF2-SC group did not show any signs of regeneration (category 4).

In the groups receiving two-chambered nerve grafts, most animals showed regenerated tissue of categories 1, 2, and 3,

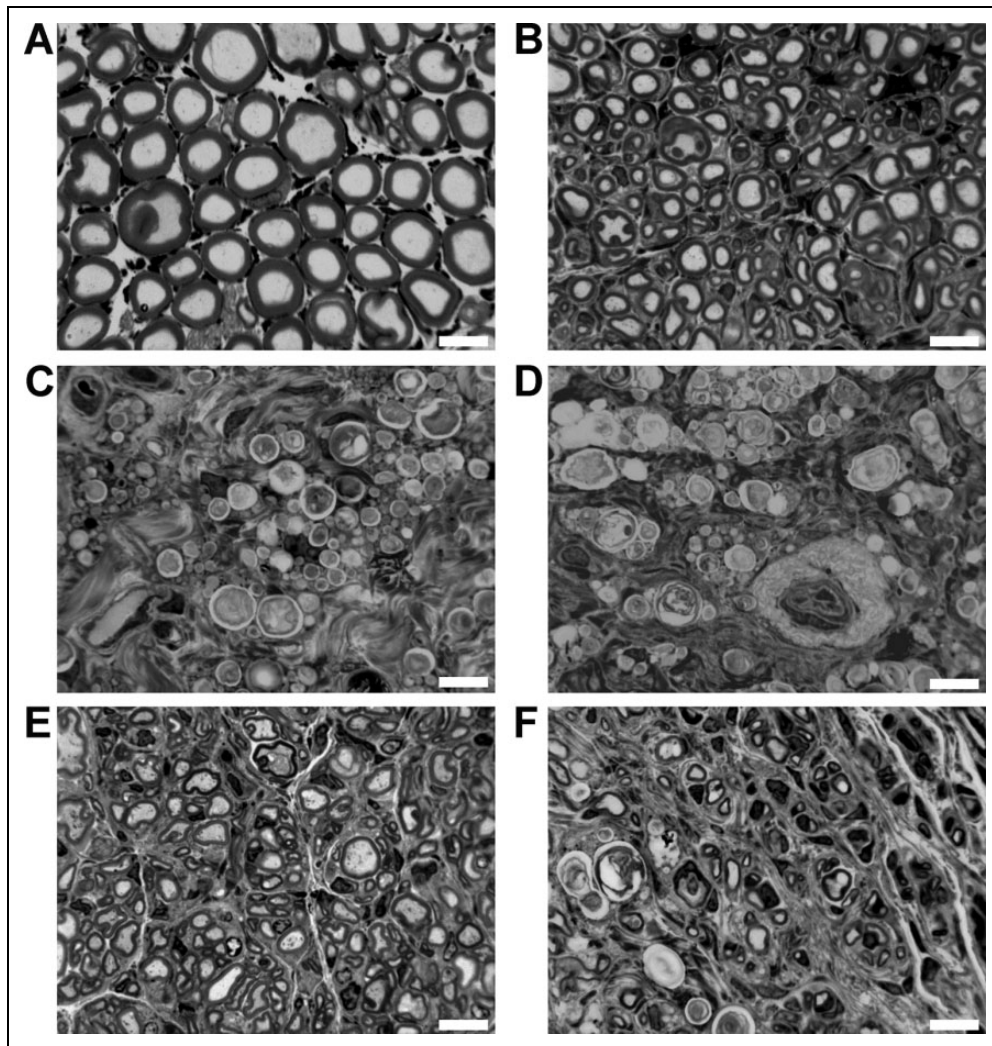


**Fig 4.** Representative pictures of toluidine blue-stained semi-thin cross-sections of distal nerve segments 120 days after reconstruction surgery. Images show healthy nerve segments (A), serving as control compared to distal nerve segments of reconstructed sciatic nerves (B–F). Examples for no axonal regeneration from (C) CNG+HAL group and (D) the CNG+HAL+fibroblast growth factor 2 (FGF2)-Schwann cell (SC) group. Examples of samples, demonstrating axonal regeneration from (B) the autologous nerve graft group, (E) the CNG[F]+HAL group, and (F) the CNG[F]+HAL+FGF2-SC group. White scale bars display 10  $\mu\text{m}$ .

except one animal of the CNG[F]+HAL group (12.5%), ending up in category 4. Eighty percent of the CNG[F]+HA and 87.5% of the CNG[F]+HAL groups regenerated two tissue cables (category 1) through the grafts. In the CNG[F]+HAL+SC group, categories 1, 2, and 3 of regenerated tissue were observed, namely category 1 in 42.9% of the animals (3/7) and category 2 and also category 3 each in 28.6% (2 of 7 animals). In the CNG[F]+HAL+FGF2-SC group, animals regenerated 2 tissue cables in 37.5% (3/8) of the animals (category 1), but most regeneration ended up in category 3 (62.5%, 5/8). Upon harvest, visible blood supply could be detected in groups, receiving two-chambered nerve grafts. The blood vessels formed within the perforations of the film.

### Nerve Histomorphometry

Healthy nerve segments as well as nerve segments, harvested distal to the grafts from differently reconstructed rat sciatic nerves, were processed into semi-thin cross-sections (Figure 4) for stereological and histomorphometrical analyses of the regenerated myelinated axons at 120 days after reconstruction surgery as shown in Table 5. All samples were included into the stereological analysis (healthy nerve:  $n = 6$ , ANG:  $n = 6$ , CNG/CNG[F]+HA:  $n = 5$ , CNG[F]+HAL+SC:  $n = 7$ , all other groups:  $n = 8$ ). Samples that revealed no axonal regeneration upon stereological analyses had to be excluded from further histomorphometrical analyses (healthy nerve:  $n = 6$ , ANG:  $n = 6$ , CNG+HA,

**Table 5.** Histomorphometrical Analyses of Healthy Controls and Distal Nerve Segments of the Reconstructed Sciatic Nerves at 120 Days Post-Surgery.

Group	Total number of myelinated fibers	Nerve fiber density (number/mm <sup>2</sup> )	Axon diameter (μm)	Fiber diameter (μm)	g-Ratio	Myelin thickness (μm)
Healthy nerve (n = 6)	6,340 ± 162.0	11,095 ± 828.8	6.12 ± 0.19	9.24 ± 0.31	0.66 ± 0.01	1.56 ± 0.07
ANG (n = 6)	5,760 ± 743.6	5,133 ± 629.6	3.88 ± 0.10	5.38 ± 0.16	0.71 ± 0.01	0.75 ± 0.05
CNG+HA	192.5 ± 189.4* (n = 5)	462.1 ± 457.0 (n = 5)	3.01 (n = 1)	4.35 (n = 1)	0.69 (n = 1)	0.67 (n = 1)
CNG+HAL	781.3 ± 508.7* (n = 8)	1,118 ± 762.7 (n = 8)	3.69	5.43	0.67	0.87
CNG+HAL+SC	4.7 ± 4.7*** (n = 8)	14.69 ± 14.69** (n = 8)	2.89 (n = 2)	4.38 (n = 2)	0.65 (n = 2)	0.74 (n = 2)
CNG+HAL+FGF2-SC	267.2 ± 267.2** (n = 8)	169.6 ± 169.6** (n = 8)	n.d. (n = 0)	n.d. (n = 0)	n.d. (n = 0)	n.d. (n = 0)
CNG[F]+HA	780 ± 308.4 (n = 5)	1,457 ± 584.7 (n = 5)	2.79 (n = 1)	3.99 (n = 1)	0.69 (n = 1)	0.60 (n = 1)
CNG[F]+HAL	1,020 ± 508.7 (n = 8)	1,840 ± 511.3 (n = 8)	2.80 ± 0.22 (n = 3)	4.02 ± 0.23 (n = 3)	0.68 ± 0.02 (n = 3)	0.61 ± 0.02 (n = 3)
CNG[F]+HAL+SC	223.2 ± 160.0 (n = 7)	252.9 ± 107.2 (n = 7)	2.96 ± 0.21 (n = 6)	4.18 ± 0.28 (n = 6)	0.70 ± 0.01 (n = 6)	0.61 ± 0.04 (n = 6)
			3.10	4.11	0.74	0.51
CNG[F]+HAL+FGF2-SC	337.5 ± 247.0 (n = 8)	314.4 ± 169.6 (n = 8)	3.01 (n = 2)	4.10 (n = 2)	0.72 (n = 2)	0.55 (n = 2)
			2.94 (n = 1)	4.05 (n = 1)	0.71 (n = 1)	0.56 (n = 1)

Total numbers of myelinated fibers (second column), nerve fiber densities (third column) as well as axon diameters (fourth column), fiber diameters (fifth column), g-ratios (sixth column), and myelin thicknesses (seventh column) are displayed. Since regeneration occurred in less than three animals per group in the CNG+HA, CNG+HAL, CNG+HAL+SC, CNG+HAL+FGF2-SC, and the CNG[F]+HAL+FGF2-SC groups (see n values), statistical analyses of histomorphometrical analyses were not applicable. When applicable, significant differences ( $P < 0.05$ ) were detected by Kruskal–Wallis test followed by Dunn's multiple comparison ( $^{*}P < 0.05$ ,  $^{**}P < 0.01$  vs. ANG). Results are presented as mean ± SEM (in cases of  $n \geq 3$ ), as mean ± SD (in cases of  $n = 2$ ), or as single values (in cases of  $n = 1$ ). ANG: autologous nerve graft; CNG: chitosan-based nerve graft; FGF-2: fibroblast growth factor 2; HA: hyaluronic acid; HAL: hyaluronic acid–laminin hydrogel; SC: Schwann cell.

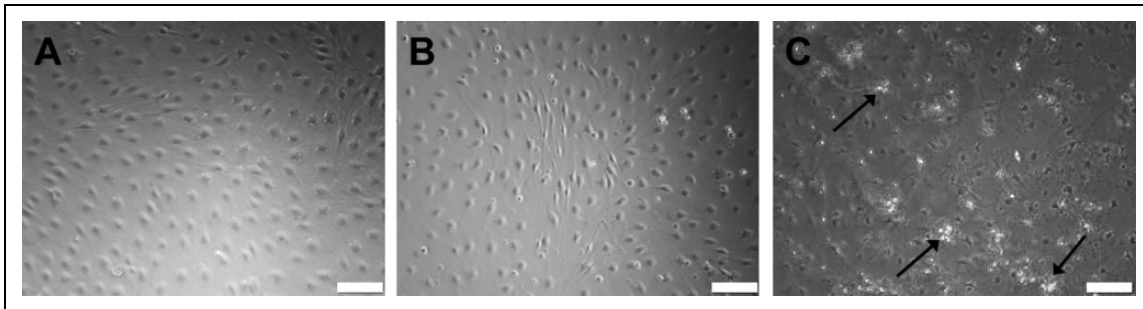
CNG+HAL+FGF2-SC, CNG[F]+HAL+FGF2-SC:  $n = 1$ , CNG+HAL, CNG[F]+HAL+SC:  $n = 2$ , CNG[F]+HA:  $n = 3$ , CNG[F]+HAL:  $n = 6$ , CNG+HAL+SC:  $n = 0$ ).

Table 5 lists the results from nerve histomorphometry. With regard to the total number of myelinated fibers (Table 5, second column) and the nerve fiber density (Table 5, third column), ANG treatment was superior to all experimental groups. Significant differences between ANG-treated animals and the CNG+HA, CNG+HAL, CNG+HAL+SC, and CNG+HAL+FGF2-SC groups could be detected concerning the total number of myelinated fibers. The ANG group also revealed a significantly higher nerve fiber density when compared to the CNG+HAL+SC and CNG+HAL+FGF2-SC groups. No significant differences were detected among the animals treated with different combinations of artificial nerve guides. However, the highest numbers of myelinated fibers as well as the highest nerve fiber densities among the artificial nerve grafts were detectable in samples from the CNG[F]+HAL group.

As axonal regeneration toward the distal nerve segment failed in many animals, a lot of samples had to be excluded from evaluation of nerve morphometry. Only ANG- ( $n = 6$ ), CNG[F]+HA- ( $n = 3$ ), and CNG[F]+HAL-treated ( $n = 6$ ) animals could be included into statistical analyses of the morphometrical parameters (Table 5, columns 4 to 7). No significant differences were detected with regard to axon diameters, fiber diameters, g-ratios, and myelin thicknesses. None of the surveyed groups recovered to healthy reference values. The highest axon and fiber diameters as well as myelin thicknesses were achieved in ANG-treated animals. Reconstruction with CNG[F]+HAL performed slightly better when compared to CNG[F]+HA concerning all tested parameters.

### Real-Time qRT-PCR

cDNA of naive SCs as well as FGF2-SCs was subjected to real-time qRT-PCR. To evaluate the regeneration supportive properties of SCs cultured in either specific SC medium (see section “Primary (Naive) Neonatal Rat SCs”), HA or HAL (see section “Preparation of 0.2% HA and 0.2% HAL”), we analyzed the expression of genes encoding for the neurotrophic factors BDNF, GDNF, NGF, and FGF-2. Representative photomicrographs show that already after culturing naive SCs within the HAL for 3 days, a lower cell density was recognizable, although initially the same cell number (350,000) was seeded in all wells (Figure 5). Consequently, it had to be assumed that differing cell numbers were available for lysis. Therefore, mRNA amounts were equalized before performing qRT-PCR analysis. The qRT-PCR results do, however, only reveal one single event of statistical significance (Figure 6E). Statistical analysis was only possible for FGF2-SCs, for which three different culture trials were enough for harvesting an appropriate amount of RNA for  $n = 3$  independent analyses. For naive SCs, however, even



**Fig 5.** Representative pictures of phase-contrast microscopy of Schwann cells (SC) seeded in either SC-specific culture medium (K<sup>+</sup>, A), hyaluronic acid (HA, B), and hyaluronic acid–laminin hydrogel (HAL, C). Three days after seeding, cells cultured in K<sup>+</sup> (A) and HA (B) showed a typical bipolar morphology. Proliferation of the initially seeded 350,000 cells led to a dense cell layer on the well ground. In HAL condition (C), SC, however, revealed a different morphology and higher apoptosis rate (cell detritus is indicated by arrows). Scale bar displays 100  $\mu$ m.

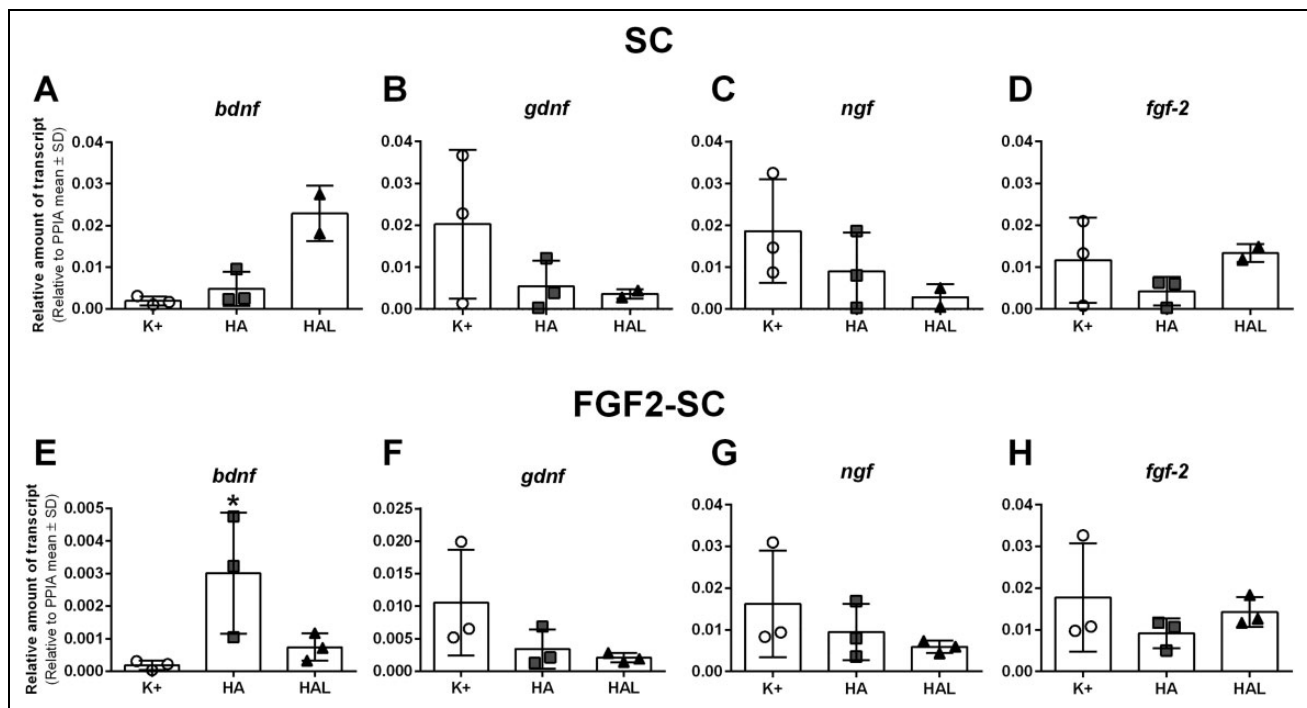


**Fig 6.** Gene expression changes in naïve Schwann cells (SCs, A-D) and fibroblast growth factor 2 (FGF2)-overexpressing Schwann cells (FGF2-SC, E-H). Gene expression of *bdnf*, *gdnf*, *ngf*, and *fgf-2* was quantified by qRT-PCR of cDNA of SCs and FGF2-SCs cultured in either specific SC medium (K<sup>+</sup>), hyaluronic acid (HA), or hyaluronic acid–laminin hydrogel (HAL). *Bdnf* is significantly higher expressed in HA-cultured FGF2-SCs when compared to K<sup>+</sup>-cultured FGF2-SCs (E). Relative amounts of transcripts to the housekeeping gene *ppia* are shown as mean  $\pm$  SD. One-way analysis of variance followed by Dunnett's multiple comparison were applied to detect significant differences (\* $P$  < 0.05 vs. K<sup>+</sup>). Naïve SCs in HAL:  $n$  = 2, rest:  $n$  = 3.

five culture trials resulted in a harvest of RNA only sufficient for pooling cDNA for  $n$  = 2 independent analyses.

Therefore, we can describe rather qualitatively that in both cell types, SCs and FGF2-SCs, *gdnf* and *ngf* were the highest expressed in the positive control and revealed the lowest expression in the HAL-cultured cells without significant differences (Figure 6B, C, F and G). Interestingly, *bdnf* showed a higher expression in both cell types cultured in HA and HAL when compared to the positive control (Figure 6A

and E). *Fgf-2* was similarly expressed in the positive control and in the HAL-cultured SCs, and was showing a slightly lower expression in SCs and FGF2-SCs cultured in HA (Figure 6D and H).

## Discussion

As outlined before, in this study we aimed to comprehensively evaluate the feasibility to use a novel HAL as a

luminal filler for hollow CNGs or two-chambered CNG[F]s. The hydrogel filler was supposed to enhance the regeneration support by providing a three-dimensional structure and hydrated milieu for the regrowing axons. Additionally, we aimed to evaluate, if HAL can serve as a carrier system for co-transplanted naïve (SCs) or neurotrophic factor delivering (FGF2-SCs) SCs. The study was performed in the 15 mm critical defect length rat sciatic nerve model, which allows state-of-the-art analysis of axonal regeneration and motor functional recovery<sup>43</sup>. The novel HAL hydrogel, applied in this study, consisted of HA and a synthetic laminin peptide, containing the sequences of two pentapeptides, found to be functionally crucial in laminin. Another ingredient was human recombinant SOD1, thought to protect against oxidative stress and known to have a synergic effect when combined with HA. Such kind of hydrogel is expected to additionally hydrate the regenerating tissue<sup>32</sup> and to create a three-dimensional matrix for improving regeneration through otherwise hollow tubular implants. In this study, we put an additional focus on the possibility to increase the regeneration-supporting activity of co-transplanted SCs when suspending them in HAL.

When evaluating the regeneration promoting potential of nerve graft developments, it is important to compare any artificial and tissue-engineered nerve guide approaches to the gold standard treatment<sup>43</sup>. Reversed ANGs were used as gold standard control in our study and proved once again to be the only graft type applied that could lead to recovery of motor function in all animals (100% recovery rate) for the TA muscle at 60 days post surgery and for the PL muscles at 90 days post surgery, as surveyed by means of electrodiagnostic measurements. Motor recovery was progressing more slowly and eventually remained incomplete until the end of the observation period in all experimental groups compared to the ANG control. When comparing the performance among the CNG groups investigated, two-chambered CNG[F]s generally performed better than hollow CNGs. This underlines our previous findings that CFs effectively guide axonal regrowth, thereby accelerating and improving functional recovery<sup>21,22,44</sup>. While for the TA muscle, the highest recovery rate was detected in the CNG[F]+HAL group (in 87.5% of the animals), the highest recovery rate for the PL muscle was detected in the CNG[F]+HA group and ranged only at 40% (two of five animals). The PL muscles are innervated by the lateral branch of the tibial nerve, one of the three branches of the sciatic nerve. In contrast to that, the TA muscle is innervated by the deep peroneal nerve, a branch from the common peroneal nerve, displaying the second branch of the sciatic nerve<sup>45,46</sup>. Besides this difference, the PL muscles are found more distally to the TA muscle, resulting in a longer distance along which the regrowing axons have to find their way back to the target tissue. The nerve repair approaches used in the current study, did, besides the ANG gold standard approach, not sufficiently support reinnervation of the PL muscles after 120 days. When having a closer look at the differences in motor

recovery and comparing the use of HA or HAL as pure luminal fillers for the nerve guides versus their use as a carrier system for co-transplanted SCs or FGF2-SCs, it is rather obvious that the additional supplementation of cells reduced the regeneration outcome in the current study.

A failure of reinnervation leads to persistent and aggravating atrophy of the target muscles, which, as performed in the current study, can be evaluated by means of MWRs<sup>43,47</sup>. The results from calculating the MWRs of two lower limb muscles, TA and GC, underscore the findings of our electrodiagnostic measurements, that none of the experimental groups achieved the values of the gold standard treatment. Among the experimental groups, highest MWRs were detected in the CNG[F]+HA group for the TA muscle and in the CNG[F]+HAL group for the GC muscle. Again, this is a hint that co-transplantation of any SC type did rather impair than support regeneration.

CMAP amplitude areas, which display the amount of reinnervating axons<sup>48</sup>, and MWRs, which display the degree of muscle atrophy or recovery<sup>47</sup>, can be directly correlated. The TA muscle was surveyed in electrodiagnostic measurements as well as by MWR calculation, leading to slightly different results in the respective tests for identical animals. In electrodiagnostic recordings the gold standard treatment group performed significantly better when compared to all experimental groups, while only TA muscle MWRs of the CNG+HAL, the CNG+HAL+SC, and the CNG+HAL+FGF2-SC groups significantly differed from those of the ANG group animals. This is resulting from the fact that CMAP amplitude areas had to be set to 0 for all animals, showing no evocable CMAP, while MWRs always include positive values even in cases of strong muscle atrophy, occurring after denervation and aggravating in cases of failed reinnervation.

Macroscopic evaluations of the regenerated tissue within the CNG or CNG[F] grafts were carried out after the end of the 120-day observation period. We could, in accordance to our previous studies, show that in CNG[F]s the regenerated tissue was very well vascularized through the perforations of the film<sup>21,22,44</sup>. The detected improved functional motor recovery in animals treated with the two-chambered CNG[F]s is very likely attributed to a better vascularization of the regrown tissue. Appropriate and timely blood vessel formation is known to play a crucial role in peripheral nerve regeneration<sup>49</sup>. Besides, CNG[F]s offer an additional mechanical longitudinal guidance structure for regrowing axons, which the CNGs are lacking.

Nerve segments harvested distal to the grafts were processed for histomorphometrical analyses. As expected, and also observed in previous other studies<sup>21,37</sup>, stereological as well as nerve morphometrical values of ANG-treated animals did not reach healthy values, but this treatment did outperform all experimental conditions evaluated. By this investigation only single events of statistical significance could be detected. Statistical differences in nerve fiber densities, however, point again toward impaired regeneration for

a co-transplantation of SCs in the HAL carrier (e.g., comparison of ANG samples versus CNG+HAL+SC and CNG+HAL+FGF2-SC samples).

The validity of nerve morphometrical analysis in the current study and the calculation of axon diameter, fiber diameter, *g*-ratio, and myelin thickness need to be considered critically. Samples from animals with no regenerated axons in the distal nerve needed to be excluded from the statistical analysis, which resulted in *n* values <3 for the groups with poor axonal regeneration (CNG+HA, CNG+HAL+FGF2-SC, CNG[F]+HAL+FGF2-SC: *n* = 1; CNG+HAL, CNG[F]+HAL+SC: *n* = 2; CNG+HAL+SC: *n* = 0). Unfortunately, the only samples that could be fully included into the statistical analysis were derived from healthy nerves and ANGs, thus drastically reducing the power of this analysis for estimating the efficacy of our artificial nerve grafting approaches.

From the current study it can be generally concluded that HA and HAL have a comparable potential to allow axonal regeneration and functional motor recovery when used as luminal hydrogel fillers for CNGs or CNG[F]s. But it also has to be considered that the regeneration outcome, e.g., for CNG+HA or CNG+HAL with a TA-CMAP recovery rate of 20% and 25%, respectively, was not as good as observed in a previous study<sup>37</sup>. The specific previous study was also performed in LEW/OrlRj rats, and we have had achieved a TA-CMAP recovery rate of 37.5% (in three of eight animals) when repairing the 15 mm sciatic nerve gap with CNGs only filled with saline upon implantation<sup>31</sup>. We have also evaluated CNG[F]s in a previous study, but back then we applied the critical defect lengths sciatic nerve repair model to RjHan:WI rats<sup>21</sup>. In this specific study the TA-CMAP recovery rate through CNG[F]s only filled with saline upon implantation was 85.7%<sup>21</sup>, which is exactly the same rate as detected in the current study in the CNG[F]-HAL group.

Therefore, we must conclude that HAL in its current formulation and how we applied it in the current study were not resulting in an overall improvement of the regeneration support that is anyway provided by the chitosan-based CNG or CNG[F] nerve guides used for critical gap lengths rat sciatic nerve repair. In the current study, the HAL was used in a final concentration of 0.2%. This concentration showed the most suitable viscosity to be transferred into the tubes safely, neither producing air pockets, nor leading to leakage from the tubes. However, by diluting the gel with cell culture medium, degradation properties may have been influenced. For offering ideal uptake and releasing mechanisms, the degradation properties of hydrogels should generally be controlled as much as possible. New studies show that controlled degradation can be used to allow the formation of growth factor gradients, thus attracting the regrowing axons and thereby successfully leading them back to the distal target tissue<sup>50</sup>. The use of hydrogels based on laminin and HA has been proposed before to enhance peripheral nerve repair<sup>25,32,51–54</sup>. In the current study, however, the randomly distributed components in the diluted HAL might not have

been sufficiently supportive for axonal guidance. In future attempts, a better alignment of hydrogel components should be aimed at. That would ideally allow the alignment of invading SCs to more easily form guidance tracks for regrowing axons<sup>55–57</sup>.

This finally leads us to the discussion of the properties of HAL, when used as a cell carrier system for co-transplantation of SCs in the current study. Upon nerve injury, local SCs undergo reprogramming, which is characterized by suppression of myelin differentiation and at the same time activation of a repair phenotype<sup>15</sup>. Consequently, myelin genes are downregulated, while markers for immature SCs are upregulated, trophic factors and cytokines released, surface proteins expressed, and autophagy of myelin debris is activated as well<sup>15</sup>. Finally, repair phenotype SCs form the Bands of Büngner functioning as regeneration tracks for axonal guidance<sup>15</sup>. To facilitate that all these will also take place inside the transplanted artificial nerve guides, it seems reasonable to suspend naïve or genetically modified SCs, already overexpressing a neurotrophic factor, in a hydrogel, as evaluated in the current study. It has been demonstrated before by us and others that transplanted SCs can survive within nerve guides for 4 to 6 weeks *in vivo*<sup>23,58</sup>. Additionally, a long-lasting effect has been postulated for regeneration-promoting proteins that have been secreted into an optimal cell carrier system by the transplanted SCs before their elimination<sup>58</sup>.

The concept of SC transplantation for increasing regeneration outcome after nerve guide repair has been successfully evaluated during the last decades. Early examples for experimental approaches have been using naïve neonatal<sup>58,59</sup> or adult<sup>60–62</sup> SCs while currently also SC lines<sup>55</sup> or genetically modified SCs delivering neurotrophic factors<sup>30,63</sup> have been investigated. Although transplantation of SCs as well as FGF2-SCs did demonstrate regeneration-supporting properties in some of our own previous studies<sup>23,25</sup>, in the current study the approach did not show any regeneration support. Instead, co-transplantation of SCs or FGF2-SCs rather reduced the recovery outcome in comparison to the application of cell-free hydrogel. This outcome was surprising to us and we aimed to get some insight into the mechanism probably responsible for this.

During preparation of the cell-transplantation approach, we had already ensured that transplantation of SCs harvested from neonatal Wistar RjHan:WI rats into adult LEW/OrlRj recipient rats would not result in a host-versus-graft reaction. This is in accordance with almost all experimental studies, we are aware of, in which SC grafts were derived from allogeneic sources (e.g.,<sup>30,55,62,64,65</sup>). We also do not think that the concentration of the co-transplanted cells was not well suitable, since we oriented toward our previous studies, where the application of  $1 \times 10^6$  cells/nerve guide was adequate for successfully supporting regeneration<sup>25</sup>.

Therefore, we hypothesized instead that when suspended in HAL, SCs and FGF2-SCs changed their gene expression profile and did consequently not sufficiently contribute to a



pro-regenerative milieu within the nerve guides. For testing this hypothesis, we monitored the appearance of SCs and FGF2-SCs under different culture conditions in vitro and further analyzed their gene expression profiles of selected neurotrophic factors under the same conditions by means of qRT-PCR. Our results demonstrate that when cultured for 3 days in HA or HAL, SCs and FGF2-SCs show a reduced cell density in comparison of cell cultures initiated with the same seeding density on control culture surface. Furthermore, culturing naïve SCs or genetically engineered FGF2-SCs within the hydrogel resulted in a relative down-regulation of genes for expressing regeneration-supportive neurotrophic factors, such as NGF and GDNF in both cell types. This indicates that HAL as well as HA could have negatively affected the secretion of regeneration-supporting proteins into the cell carrier system. Thereby the grafted cells may also have changed the milieu inside the nerve guide toward an environment that reduced invasion of host repair SCs and regrowing axons that would follow them. Also, when the survival of the co-transplanted cells was not secured by the surrounding milieu, they may have undergone apoptosis and their detritus material might have displayed a hindrance for the regrowing axons<sup>21</sup>.

## Conclusion

The design of bioartificial nerve grafts with the aim to imitate structure and properties of physiological nerve tissue as provided with ANGs is under continuous progress. The study presented here was designed in the positive anticipation that the combination of CNGs or CNG[F]s with HAL and FGF2-SCs, which have individually proven before to exert beneficial impacts on the process of peripheral nerve regeneration across critical lengths defects, would significantly improve and accelerate functional motor recovery. The results of our comprehensive in vivo and in vitro analyses, however, clearly revealed that neither HAL as a pure luminal filler, nor in combination with co-transplanted SCs could add on to the very good regeneration-supporting properties of CNGs and particularly CNG[F]s. Moreover, we detected a negative interference between the suspended cells and the proposed cell carrier system in our co-transplantation approach. In future studies, the administration of ECM components should be more specifically tuned toward either supporting invasion of host repair SCs and facilitating axonal regrows, e.g., boosting the host repair system, or toward optimization of a cell carrier system for grafting supportive cells.

## Acknowledgments

For their excellent technical assistance, we thank Jennifer Metzen, Silke Fischer, and Natascha Heidrich from the Institute of Neuroanatomy and Cell Biology.

## Author Contributions

KHT, SR, and MA contributed to conception and design of the study; ND and KHT conducted the experiments; ZN, SR, and

MA developed and produced the hyaluronic acid–laminin hydrogel, ND evaluated the functional recovery and conducted the histomorphometrical evaluation, organized the respective data presentation; TL performed and evaluated the in vitro analysis of immunocompatibility between recipient spleen and lymph node cells and donor Schwann cells; SK, ZH, and TS conducted primer design, cell culture experiments, and PCR analysis for evaluation of hydrogel impact on suspended cells; ND performed the statistical data analysis for all experimental parts; ND and KHT wrote the first draft of the manuscript. All authors contributed to critical reading and manuscript revision, and read and approved the submitted version.

## Availability of Research Data

The datasets analyzed during this study are available from the corresponding author on request. Raw data are stored in the authors' institutional repositories and will be accordingly provided upon request.

## Ethical Approval

All animal experiments, performed in this study, were conducted in accordance with the German animal protection law and with the European Communities Council Directive 2010/63/EU for the protection of animals used for experimental purposes. All experiments were approved by the Local Institutional Animal Care and Research Advisory and the animal care committee of Lower-Saxony, Germany (approval code: 33.12 42502-04-16/2320; approval date: 30.11.2016).

## Statement of Human and Animal Rights

All animal procedures were performed according to protocols Local Institutional Animal Care and Research Advisory and the animal care committee of Lower-Saxony, Germany. Human subjects were not used in this study.

## Statement of Informed Consent

There are no human subjects in this article and informed consent is not applicable.

## Declaration of Conflicting Interests

The author(s) declared no potential conflicts of interest with respect to the research, authorship, and/or publication of this article.

## Funding

The author(s) disclosed receipt of the following financial support for the research, authorship, and/or publication of this article: Financial support was provided (1) by the German Israeli Foundation for Scientific Research and Development (G-1350-409.10\_2016, to KHT) and (2) the Konrad Adenauer Stiftung (to ND).

## ORCID iD

Nina Dietzmeyer  <https://orcid.org/0000-0003-3835-7606>

## Supplemental Material

Supplemental material for this article is available online.

## References

- Asplund M, Nilsson M, Jacobsson A, von Holst H. Incidence of traumatic peripheral nerve injuries and amputations in Sweden between 1998 and 2006. *Neuroepidemiology*. 2009;32(3):217–228.
- Noble J, Munro CA, Prasad VS, Midha R. Analysis of upper and lower extremity peripheral nerve injuries in a population of patients with multiple injuries. *J Trauma*. 1998;45(1):116–122.
- Eriksson M, Karlsson J, Carlsson KS, Dahlin LB, Rosberg HE. Economic consequences of accidents to hands and forearms by log splitters and circular saws: cost of illness study. *J Plast Surg Hand Surg*. 2011;45(1):28–34.
- Deumens R, Bozkurt A, Meek MF, Marcus MA, Joosten EA, Weis J, Brook GA. Repairing injured peripheral nerves: bridging the gap. *Prog Neurobiol*. 2010;2010(3):245–276.
- Grinsell D, Keating CP. Peripheral nerve reconstruction after injury: a review of clinical and experimental therapies. *Biomed Res Int*. 2014;2014:698256.
- Daly W, Yao L, Zeugolis D, Windebank A, Pandit A. A biomaterials approach to peripheral nerve regeneration: bridging the peripheral nerve gap and enhancing functional recovery. *J R Soc Interface*. 2012;9(67):202–221.
- Dietzmeier N, Förthmann M, Grothe C, Haastert-Talini K. Modification of tubular chitosan-based peripheral nerve implants – applications for simple or more complex approaches. *Neural Regen Res*. 2019;15(8):1421–1431.
- Kornfeld T, Vogt PM, Radtke C. Nerve grafting for peripheral nerve injuries with extended defect sizes. *Wien Med Wochenschr*. 2019;169(9-10):240–251.
- Bell JH, Haycock JW. Next generation nerve guides: materials, fabrication, growth factors, and cell delivery. *Tissue Eng Part B Rev*. 2012;18(2):116–128.
- Kehoe S, Zhang XF, Boyd D. Fda approved guidance conduits and wraps for peripheral nerve injury: a review of materials and efficacy. *Injury*. 2012;43(5):553–572.
- Dalamagkas K, Tsintou M, Seifalian A. Advances in peripheral nervous system regenerative therapeutic strategies: a biomaterials approach. *Mater Sci Eng C Mater Biol Appl*. 2016;65:425–432.
- Fairbairn NG, Meppelink AM, Ng-Glazier J, Randolph MA, Winograd JM. Augmenting peripheral nerve regeneration using stem cells: a review of current opinion. *World J Stem Cells*. 2015;7(1):11–26.
- Lackington WA, Ryan AJ, O'Brien FJ. Advances in nerve guidance conduit-based therapeutics for peripheral nerve repair. *ACS Biomaterials Science & Engineering*. 2017;3(7):1221–1235.
- Gaudet AD, Popovich PG, Ramer MS. Wallerian degeneration: gaining perspective on inflammatory events after peripheral nerve injury. *J Neuroinflammation*. 2011;8:110.
- Jessen KR, Mirsky R. The repair Schwann cell and its function in regenerating nerves. *J Physiol*. 2016;594(13):3521–3531.
- Gonzalez-Perez F, Udina E, Navarro X. Extracellular matrix components in peripheral nerve regeneration. *Int Rev Neurobiol*. 2013;108:257–275.
- Jessen KR, Mirsky R, Lloyd AC. Schwann cells: development and role in nerve repair. *Cold Spring Harb Perspect Biol*. 2015;7(7):a020487.
- Haastert-Talini K, Geuna S, Dahlin LB, Meyer C, Stenberg L, Freier T, Heimann C, Barwig C, Pinto LF, Raimondo S, Gambarotta G, et al. Chitosan tubes of varying degrees of acetylation for bridging peripheral nerve defects. *Biomaterials*. 2013;34(38):9886–9904.
- Shapira Y, Tolmasov M, Nissan M, Reider E, Koren A, Biron T, Bitan Y, Livnat M, Ronchi G, Geuna S, Rochkind S. Comparison of results between chitosan hollow tube and autologous nerve graft in reconstruction of peripheral nerve defect: an experimental study. *Microsurgery*. 2016;36(8):664–671.
- Gonzalez-Perez F, Cobiañchi S, Geuna S, Barwig C, Freier T, Udina E, Navarro X. Tubulization with chitosan guides for the repair of long gap peripheral nerve injury in the rat. *Microsurgery*. 2015;35(4):300–308.
- Meyer C, Stenberg L, Gonzalez-Perez F, Wrobel S, Ronchi G, Udina E, Suganuma S, Geuna S, Navarro X, Dahlin LB, Grothe C, et al. Chitosan-film enhanced chitosan nerve guides for long-distance regeneration of peripheral nerves. *Biomaterials*. 2016;76:33–51.
- Stenberg L, Stöbel M, Ronchi G, Geuna S, Yin Y, Mommert S, Martensson L, Metzén J, Grothe C, Dahlin LB, Haastert-Talini K. Regeneration of long-distance peripheral nerve defects after delayed reconstruction in healthy and diabetic rats is supported by immunomodulatory chitosan nerve guides. *BMC Neurosci*. 2017;18(1):53.
- Haastert K, Lipokatic E, Fischer M, Timmer M, Grothe C. Differentially promoted peripheral nerve regeneration by grafted Schwann cells over-expressing different fgf-2 isoforms. *Neurobiol Dis*. 2006;21(1):138–153.
- Haastert K, Mauritz C, Matthies C, Grothe C. Autologous adult human Schwann cells genetically modified to provide alternative cellular transplants in peripheral nerve regeneration. *J Neurosurg*. 2006;104(5):778–786.
- Meyer C, Wrobel S, Raimondo S, Rochkind S, Heimann C, Shahar A, Ziv-Polat O, Geuna S, Grothe C, Haastert-Talini K. Peripheral nerve regeneration through hydrogel-enriched chitosan conduits containing engineered Schwann cells for drug delivery. *Cell Transplant*. 2016;25(1):159–182.
- Grothe C, Nikkhah G. The role of basic fibroblast growth factor in peripheral nerve regeneration. *Anat Embryol (Berl)*. 2001;204(3):171–177.
- Jungnickel J, Haase K, Konitzer J, Timmer M, Grothe C. Faster nerve regeneration after sciatic nerve injury in mice over-expressing basic fibroblast growth factor. *J Neurobiol*. 2006;66(9):940–948.
- Grothe C, Haastert K, Jungnickel J. Physiological function and putative therapeutic impact of the fgf-2 system in peripheral nerve regeneration—lessons from in vivo studies in mice and rats. *Brain Res Brain Res Rev*. 2006;51(2):293–299.
- Aebischer P, Guenard V, Brace S. Peripheral nerve regeneration through blind-ended semipermeable guidance channels: effect of the molecular weight cutoff. *J Neurosci*. 1989;9(10):3590–3595.

30. Allodi I, Mecollari V, Gonzalez-Perez F, Eggers R, Hoyng S, Verhaagen J, Navarro X, Udina E. Schwann cells transduced with a lentiviral vector encoding fgf-2 promote motor neuron regeneration following sciatic nerve injury. *Glia*. 2014;62(10):1736–1746.
31. Grothe C, Timmer M. The physiological and pharmacological role of basic fibroblast growth factor in the dopaminergic nigrostriatal system. *Brain Res Rev*. 2007;54(1):80–91.
32. Rochkind S, Nevo Z. Recovery of peripheral nerve with massive loss defect by tissue engineered guiding regenerative gel. *Biomed Res Int*. 2014;2014:327578.
33. Haastert K, Grosskreutz J, Jaeckel M, Laderer C, Bufler J, Grothe C, Claus P. Rat embryonic motoneurons in long-term co-culture with Schwann cells—a system to investigate motoneuron diseases on a cellular level in vitro. *J Neurosci Methods*. 2005;142(2):275–284.
34. Ratzka A, Baron O, Grothe C. Fgf-2 deficiency does not influence fgf ligand and receptor expression during development of the nigrostriatal system. *PLoS One*. 2011;6(8): e23564.
35. Ratzka A, Kalve I, Ozer M, Nobre A, Wesemann M, Jungnickel J, Koster-Patzlaff C, Baron O, Grothe C. The colayer method as an efficient way to genetically modify mesencephalic progenitor cells transplanted into 6-ohda rat model of Parkinson's disease. *Cell Transplant*. 2012;21(4):749–762.
36. Rumpel R, Alam M, Klein A, Ozer M, Wesemann M, Jin XX, Krauss JK, Schwabe K, Ratzka A, Grothe C. Neuronal firing activity and gene expression changes in the subthalamic nucleus after transplantation of dopamine neurons in hemiparkinsonian rats. *Neurobiology of Disease*. 2013;59:230–243.
37. Stöbel M, Wildhagen VM, Helmecke O, Metzen J, Pfund CB, Freier T, Haastert-Talini K. Comparative evaluation of chitosan nerve guides with regular or increased bendability for acute and delayed peripheral nerve repair: a comprehensive comparison with autologous nerve grafts and muscle-in-vein grafts. *Anat Rec (Hoboken)*. 2018;301(10):1697–1713.
38. Stöbel M, Metzen J, Wildhagen VM, Helmecke O, Rehra L, Freier T, Haastert-Talini K. Long-term in vivo evaluation of chitosan nerve guide properties with respect to two different sterilization methods. *Biomed Res Int*. 2018;2018:6982738.
39. Navarro X, Buti M, Verdu E. Autotomy prevention by amitriptyline after peripheral nerve section in different strains of mice. *Restor Neurol Neurosci*. 1994;6(2):151–157.
40. Korte N, Schenk HC, Grothe C, Tipold A, Haastert-Talini K. Evaluation of periodic electrodiagnostic measurements to monitor motor recovery after different peripheral nerve lesions in the rat. *Muscle Nerve*. 2011;44(1):63–73.
41. Stöbel M, Rehra L, Haastert-Talini K. Reflex-based grasping, skilled forelimb reaching, and electrodiagnostic evaluation for comprehensive analysis of functional recovery – the 7 mm rat median nerve gap repair model revisited. *Brain Behav*. 2017;7(10):e00813.
42. Geuna S, Tos P, Battiston B, Guglielmo R. Verification of the two-dimensional disector, a method for the unbiased estimation of density and number of myelinated nerve fibers in peripheral nerves. *Ann Anat*. 2000;182(1):23–34.
43. Navarro X. Functional evaluation of peripheral nerve regeneration and target reinnervation in animal models: a critical overview. *Eur J Neurosci*. 2016;43(3):271–286.
44. Dietzmeyer N, Forthmann M, Leonhard J, Helmecke O, Brandenberger C, Freier T, Haastert-Talini K. Two-chambered chitosan nerve guides with increased bendability support recovery of skilled forelimb reaching similar to autologous nerve grafts in the rat 10 mm median nerve injury and repair model. *Front Cell Neurosci*. 2019;13:149.
45. Swett JE, Wikholm RP, Blanks RH, Swett AL, Conley LC. Motoneurons of the rat sciatic nerve. *Exp Neurol*. 1986;93(1):227–252.
46. Schmalbruch H. Fiber composition of the rat sciatic nerve. *Anat Rec*. 1986;215(1):71–81.
47. Evans PJ, Mackinnon SE, Best TJ, Wade JA, Awerbuck DC, Makino AP, Hunter DA, Midha R. Regeneration across preserved peripheral nerve grafts. *Muscle Nerve*. 1995;18(10):1128–1138.
48. Cudston PA. Electrophysiology in neuromuscular disease. *Vet Clin North Am Small Anim Pract*. 2002;32(1):31–62.
49. Penkert G, Bini W, Samii M. Revascularization of nerve grafts: an experimental study. *J Reconstr Microsurg*. 1988;4(4):319–325.
50. Hsu R-S, Chen P-Y, Fang J-H, Chen Y-Y, Chang C-W, Lu Y-J, Hu S-H. Adaptable microporous hydrogels of propagating ngf-gradient by injectable building blocks for accelerated axonal outgrowth. *Advanced Science*. 2019;6(16):1900520.
51. Madison RD, da Silva C, Dikkes P, Sidman RL, Chiu TH. Peripheral nerve regeneration with entubulation repair: comparison of biodegradable nerve guides versus polyethylene tubes and the effects of a laminin-containing gel. *Exp Neurol*. 1987;95(2):378–390.
52. Verdu E, Labrador RO, Rodriguez FJ, Ceballos D, Fores J, Navarro X. Alignment of collagen and laminin-containing gels improve nerve regeneration within silicone tubes. *Restor Neurol Neurosci*. 2002;20(5):169–179.
53. Wang KK, Nemeth IR, Seckel BR, Chakalis-Haley DP, Swann DA, Kuo JW, Bryan DJ, Cetrulo CL, Jr. Hyaluronic acid enhances peripheral nerve regeneration in vivo. *Microsurgery*. 1998;18(4):270–275.
54. Li R, Liu H, Huang H, Bi W, Yan R, Tan X, Wen W, Wang C, Song W, Zhang Y, Zhang F, et al. Chitosan conduit combined with hyaluronic acid prevent sciatic nerve scar in a rat model of peripheral nerve crush injury. *Mol Med Rep*. 2018;17(3):4360–4368.
55. Georgiou M, Bunting SC, Davies HA, Loughlin AJ, Golding JP, Phillips JB. Engineered neural tissue for peripheral nerve repair. *Biomaterials*. 2013;34(30):7335–7343.
56. Gonzalez-Perez F, Hernandez J, Heimann C, Phillips JB, Udina E, Navarro X. Schwann cells and mesenchymal stem cells in laminin- or fibronectin-aligned matrices and regeneration across a critical size defect of 15 mm in the rat sciatic nerve. *J Neurosurg Spine*. 2018;28(1):109–118.
57. Du J, Liu J, Yao S, Mao H, Peng J, Sun X, Cao Z, Yang Y, Xiao B, Wang Y, Tang P, et al. Prompt peripheral nerve regeneration

- induced by a hierarchically aligned fibrin nanofiber hydrogel. *Acta Biomater.* 2017;55:296–309.
58. Mosahebi A, Fuller P, Wiberg M, Terenghi G. Effect of allogeneic Schwann cell transplantation on peripheral nerve regeneration. *Exp Neurol.* 2002;173(2):213–223.
  59. Hadlock T, Sundback C, Hunter D, Cheney M, Vacanti JP. A polymer foam conduit seeded with Schwann cells promotes guided peripheral nerve regeneration. *Tissue Eng.* 2000;6(2):119–127.
  60. Guenard V, Kleitman N, Morrissey TK, Bunge RP, Aebischer P. Syngeneic Schwann cells derived from adult nerves seeded in semipermeable guidance channels enhance peripheral nerve regeneration. *J Neurosci.* 1992;12(9):3310–3320.
  61. Ansselin AD, Fink T, Davey DF. Peripheral nerve regeneration through nerve guides seeded with adult Schwann cells. *Neuro-pathol Appl Neurobiol.* 1997;23(5):387–398.
  62. Rodriguez FJ, Verdu E, Ceballos D, Navarro X. Nerve guides seeded with autologous Schwann cells improve nerve regeneration. *Exp Neurol.* 2000;161(2):571–584.
  63. Mason MR, Tannemaat MR, Malesy MJ, Verhaagen J. Gene therapy for the peripheral nervous system: a strategy to repair the injured nerve?. *Curr Gene Ther.* 2011;11(2):75–89.
  64. Evans GR, Brandt K, Katz S, Chauvin P, Otto L, Bogle M, Wang B, Meszlenyi RK, Lu L, Mikos AG, Patrick CW. Bioactive poly(l-lactic acid) conduits seeded with Schwann cells for peripheral nerve regeneration. *Biomaterials.* 2002;23(3):841–848.
  65. Haastert-Talini K, Schaper-Rinkel J, Schmitte R, Bastian R, Muhlenhoff M, Schwarzer D, Draeger G, Su Y, Scheper T, Gerardy-Schahn R, Grothe C. In vivo evaluation of polysialic acid as part of tissue-engineered nerve transplants. *Tissue Eng Part A.* 2010;16(10):3085–3098.